

Adaptive Bayesian Inference for Discontinuous Inverse Problems, Application to Hyperbolic Conservation Laws

Alexandre Birolleau^{1,2}, Gaël Poëtte¹ and Didier Lucor^{2,3,*}

¹ CEA, DAM, DIF, F-91297 Arpajon, France.

² UPMC Univ Paris 06, UMR 7190, Institut Jean Le Rond d'Alembert, F-75005 Paris, France.

³ CNRS, UMR 7190, Institut Jean Le Rond d'Alembert, F-75005 Paris, France.

Received 24 January 2013; Accepted (in revised version) 7 November 2013

Available online 28 March 2014

Abstract. Various works from the literature aimed at accelerating Bayesian inference in inverse problems. Stochastic spectral methods have been recently proposed as surrogate approximations of the forward uncertainty propagation model over the support of the prior distribution. These representations are efficient because they allow affordable simulation of a large number of samples from the posterior distribution. Unfortunately, they do not perform well when the forward model exhibits strong nonlinear behavior with respect to its input.

In this work, we first relate the fast (exponential) L^2 -convergence of the forward approximation to the fast (exponential) convergence (in terms of Kullback-Leibler divergence) of the approximate posterior. In particular, we prove that in case the prior distribution is *uniform*, the posterior is at least twice as fast as the convergence rate of the forward model in those norms. The Bayesian inference strategy is developed in the framework of a stochastic spectral projection method. The predicted convergence rates are then demonstrated for simple nonlinear inverse problems of varying smoothness.

We then propose an efficient numerical approach for the Bayesian solution of inverse problems presenting strongly nonlinear or discontinuous system responses. This comes with the improvement of the forward model that is *adaptively* approximated by an iterative generalized Polynomial Chaos-based representation. The numerical approximations and predicted convergence rates of the former approach are compared to the new iterative numerical method for nonlinear time-dependent test cases of varying dimension and complexity, which are relevant regarding our hydrodynamics motivations and therefore regarding hyperbolic conservation laws and the apparition of discontinuities in finite time.

AMS subject classifications: 52B10, 65D18, 68U05, 68U07

Key words: Stochastic inverse problems, Bayesian inference, iterative generalized Polynomial Chaos, compressible gas dynamics.

*Corresponding author. *Email addresses:* alexandre.birolleau@cea.fr (A. Birolleau), gael.poette@cea.fr (G. Poëtte), didier.lucor@upmc.fr (D. Lucor)

1 Introduction

Nowadays, the development of efficient computational tools to support decision-making and risk analysis under *uncertainty* is critical for the design and operation of engineered systems and more generally for *reliable* predictive science. An open question with a huge significance for *uncertainty quantification* (UQ) is the problem of realistic representation of *input* uncertainty (initial/operating/boundary conditions, model parameters, source terms, ...) to the model. A quick survey of the UQ literature shows that research in this area has been accustomed to the development of the propagation step and quantification of the response, with improvement on the efficiency, implementation, performance, ... In many works, the quantification of input uncertainty is often rudimentary, associating a random variable to each of the random parameter, and often making *a priori* choice on the distributions, relying for instance on *labelled* distributions, such as *uniform* distributions, due to a lack of knowledge. Another weakness is the assumption of random parameters *independence*. Indeed, the *gold rush* for the development of suitable and efficient stochastic representations of ever increasing larger data sets (e.g., hundreds of random parameters) relies heavily on the assumption of independent random dimensions which is most of the time not justified for engineering systems. In fact the effective stochastic dimensionality of the system depends strongly on the appropriate representation of the correlations existing between the dependent random variables representing the inputs. This mathematical description is particularly difficult when data is gathered from different sources, let say from both experiments and simulations, or when direct observations/measurements are not possible or too costly. Several methodologies for the identification of representations of random variables/processes from *experimental* data for instance have been proposed, such as the method of moments [2], maximum likelihood [8, 17], maximum entropy [7] or Bayesian inference [16, 77]. Inverse problems (IP) usually refer to the estimation of model parameters or inputs from *indirect* observations. While the resolution of a forward model predicts the system outputs given the inputs by solving the governing equations, the IP reverses this relationship by seeking to estimate uncertain inputs from measurements or observations. The IP is often formulated as a (large) *deterministic nonlinear* optimization problem that minimizes the discrepancy between the observed and predicted outputs in some appropriate norm while also minimizing a regularization term that penalizes unwanted features of the inputs [27, 65]. Following this procedure, a set of *best* inputs, i.e., fitting the data and minimizing the regularization penalty term, are obtained. Nevertheless, the predictive accuracy strongly depends on the availability of large input data sets. In practice the observations are *limited* and often *noisy*. Therefore, it becomes more legitimate to seek a complete *statistical* description of the input values that is consistent with the data, instead of discrete estimates of the best-fit inputs.

The Bayesian inference follows this path by reformulating the IP as a problem of *statistical inference*, incorporating the forward model, prior information on the inputs, and uncertainties in the measurements. The solution is the *posterior* joint pdf of the inputs,

which reflects the degree of confidence in their values [27, 66]. However, it remains challenging to use this approach for problems with high-dimensional spaces due to the requirement of solving the forward model at every sample point. In order to alleviate this problem, several sampling-based approaches have been proposed, one of the most successful being the Markov Chain Monte-Carlo (MCMC). MCMC covers a broad range of methods for numerically computing probabilities, or for optimization [12, 13, 18, 50, 60]. They are simulation methods, mostly used in complex stochastic systems where exact computation are not computationally feasible. Methods that fall under this heading include *Metropolis* sampling, *Hastings* sampling and *Gibbs* sampling.

More recent works have explored the use of forward *surrogate* models to accelerate the convergence of robust optimization (e.g., [36]) or Bayesian inference [10, 45]. In particular, Marzouk et al. [43–45] were precursors of the use of spectral methods, taking advantages of stochastic spectral representations (such as Polynomial Chaos approximations) for forward uncertainty propagation. They show that the use of the generalized Polynomial Chaos (gPC) methods seems promising to improve the acceleration of stochastic inverse problems and broaden their scope. But they also point to overwhelming difficulties in the case of discontinuous solutions in the physical and the stochastic spaces, see also [1, 32, 74]. They show that due to the poor approximation of solutions with low regularity, the gPC representation induces some errors that are propagated and amplified to the input parameter posterior distribution via measurement errors.

Indeed, for strongly nonlinear hyperbolic problems, such as compressible fluid/gas dynamics, aeroelastic flutter, multi-phase and/or reacting flows, etc., standard polynomial chaos reconstruction of the system response fails because of the occurrence of Gibbs oscillations due to the lack of smoothness. In this case, one may rely on adaptive procedures. The first attempt of model adaptation was achieved by *multiresolution/multiscale* schemes (e.g., wavelets and multi-wavelets) [31], soon followed by random *partitioning* with *a posteriori* heuristic convergence criteria [72]. Later, complementary approaches were proposed with random/spatial spaces *partitioning* [28, 46, 76] (with dual-based error estimation techniques to improve global error estimation) or *hierarchical sparse grid collocation* [39] and more recently, *binary trees* [69]. Other original approaches such as *hp*-adaptive piecewise gPC representation [34], *nonlinear Galerkin-type* formulation [54, 56], or *hybrid* approaches [55, 57] were also proposed. In this paper, we will approximate the forward problem with an iterative approach for Galerkin-based spectral projection methods called iterative-gPC (i-gPC). It was recently introduced [58] and was shown to be more accurate than the classical approach (with the same level of approximation) especially when nonlinear transformations of random variables are in play.

The paper is organized as follows: Section 2 presents the inverse problem formulation and solution approach via accelerated Bayesian inference through the use of stochastic spectral methods, while Section 3 briefly introduces gPC and i-gPC representation of random variables and processes in the framework of a stochastic spectral projection method. In Section 4, we prove a theoretical result emphasizing the relevance of recurring to L^2 -convergent approximation in order to accelerate Bayesian Inference. The efficiency of the

combination is then put forward in Section 5. Numerical approximations and predicted convergence rates are illustrated for some nonlinear and time-dependent test cases of varying dimension and complexity, which are relevant regarding our hydrodynamics motivations and therefore regarding hyperbolic conservation laws and the apparition of discontinuities in finite time.

2 Statistical inverse problems

In this paper, we focus on Bayesian inference for inverse problems on an unknown parameter of finite dimension ($\theta \in \mathbb{R}^d$). The purpose is, at the end, to provide an estimation of the parameter θ .

Bayesian inference theory is based upon Bayes' formula. This is an inversion formula for conditional probabilities. In the case of Bayesian statistical inverse problems, we are interested in inferring on θ , our parameter of interest, knowing experimental data m . Thus, we want to compute $\mathbb{P}(\theta|m)$ (the posterior). By Bayes' theorem, we get the posterior

$$\mathbb{P}(\theta|m) \propto \mathbb{P}(\theta)\mathbb{P}(m|\theta). \quad (2.1)$$

The notation $\pi_{\text{post}}(\theta)$ for the posterior $\mathbb{P}(\theta|m)$ and $\pi_{\text{pr}}(\theta)$ for the prior $\mathbb{P}(\theta)$ are common and will be used in this paper. We have, here, to make an assumption to compute the likelihood $\mathbb{P}(m|\theta)$, which describes the confidence on the measures. In this paper, it is assumed to be given by experimentalists, but it may also be dealt with into the Bayesian inference.

The basic hypothesis we make is to consider an additive relationship between the data m_x at point x , the direct model $u(x;\theta)$ given θ , and the measurement error ε ,

$$m_x = u(x;\theta) + \varepsilon, \quad (2.2)$$

with ε following the pdf π_ε , which is independent of x . This hypothesis is widely used in the literature, see for example in [20, 29]. In this case, the measurement error is chosen Gaussian, i.e., $\pi_\varepsilon = \mathcal{N}(0, \sigma^2)$, with a standard deviation σ related to the experimental device. From Eq. (2.2), we get the model for $\mathbb{P}(m|\theta)$:

$$\mathbb{P}(m|\theta) = \pi_\varepsilon(m_x - u(x;\theta)). \quad (2.3)$$

The initial information about θ is translated into the prior pdf π_{pr} . How this translation is performed is a great issue for Bayesian inference. For example, it may be a uninformative prior, from a previous study, from empirical Bayes method, or deduced according to the maximum entropy principle [23, 24]. In this paper, we consider only simple *uniform* priors and we refer the readers to [3, 22, 84] and the Chapter 3 in [61] for more details about prior selections.

Assuming that we have N independent measures, $\{m_{x_1}, \dots, m_{x_N}\}$ at points $\{x_1, \dots, x_N\}$ and using the Eqs. (2.3) and (2.1), we get the posterior probability function

$$\pi_{\text{post}}(\theta) = \frac{1}{\gamma} \pi_{\text{pr}}(\theta) \prod_{i=1}^N \pi_{\varepsilon}(m_{x_i} - u(x_i; \theta)), \quad (2.4)$$

with

$$\gamma = \int_{\theta} \pi_{\text{pr}}(\theta) \prod_{i=1}^N \pi_{\varepsilon}(m_{x_i} - u(x_i; \theta)) \, d\theta. \quad (2.5)$$

The probability density function π_{post} contains all the information we have, both from experimental data and from previous knowledge. It represents our state of knowledge.

For most practical cases, such as fluid mechanics simulations, the numerical resolution of the direct model u is too computationally intensive and makes the resolution of (2.4) intractable. The following papers [40–42, 44] have suggested using an approximate surrogate model instead, so that each measure i , $\theta \mapsto u(x_i; \theta) \triangleq u_i(\theta)$ is replaced by an approximate model $\theta \mapsto \tilde{u}_i(\theta)$. In this case, one obtains an approximate posterior,

$$\tilde{\pi}_{\text{post}}(\theta) = \frac{1}{\gamma_n} \pi_{\text{pr}}(\theta) \prod_{i=1}^N \pi_{\varepsilon}(m_{x_i} - \tilde{u}_{n,i}(\theta)), \quad (2.6)$$

where n denotes the truncature order of the representation and γ_n is normalization coefficient of the surrogate approximation see (2.6).

In the following section, we will briefly introduce several options for surrogate models in the form of stochastic spectral approximations based on Polynomial Chaos theory.

3 Stochastic spectral representations of the forward model

In the following sections, we will briefly review standard and iterative generalized Polynomial Chaos (gPC) approximations, focusing on the differences between the two approaches in the context of *non linear* transformations possibly leading to *discontinuous* solutions.

3.1 Generalized Polynomial Chaos

The Polynomial Chaos (PC) is a non-statistical representation used to approximate random variables [78], as well as to solve stochastic differential and partial differential equations (SPDE) [15, 33, 83] and it has been used for several classes of computational fluid mechanics (CFD), e.g., heat transfer, thermofluidics, porous media flows, incompressible and reacting problems, shock-dominated compressible flows, shear flows, flow-structure interactions, flows in random geometry, turbulence and uncertain unsteady dynamics,

... It is based on the Cameron-Martin's convergence theorem [5] which can be understood as a generalization of Weierstrass's for arbitrary probability measures. Let $(H_k)_{k \in \mathbb{N}}$ denote the normalized d -dimensional Hermite polynomials. Let Ξ denote a centered d -dimensional normalized Gaussian random variable. The ensemble $(H_i(\Xi))_{i \in \mathbb{N}}$ forms an orthonormal basis of $L^2(\Theta, \mathcal{B}, \mathbb{P})$, see [5]. The result is the following: let $(u(\theta))_{\theta \in \Theta}$ be a random variable in $L^2(\Theta, \mathcal{B}, \mathbb{P})$, then

$$\boxed{u^{\mathbb{P}}(\theta) = \sum_{k=0}^{\mathbb{P}} u_k H_k(\Xi(\theta)) \xrightarrow[\mathbb{P} \rightarrow \infty]{L^2(\Theta, \mathcal{B}, \mathbb{P})} u(\theta)}, \quad (3.1)$$

where the deterministic coefficients $(u_k)_{k \in \mathbb{N}}$ are projection of $u(\theta)$ on the basis. We have:

$$u_k = \int_{\theta \in \Theta} u(\theta) H_k(\Xi(\theta)) d\mathbb{P}(\theta). \quad (3.2)$$

Convergence is in the $L^2(\Theta, \mathcal{B}, \mathbb{P})$ -sense and is exponential. Moreover, it is optimal for Gaussian $u(\theta)$. In the case of non-Gaussian random variables, gPC was introduced [81] and applied in order to ameliorate the convergence rate, see among others [37, 47, 49, 51, 64, 75, 82].

3.2 Iterative generalized Polynomial Chaos

The i-gPC approximation, first introduced in [58], is an *adaptive* moment-based method [26, 48] generalizing the gPC representation. It is inspired by the work of Wiener [79] and Gerritsma et al. [14, 71]. It is particularly efficient for *discontinuous* dependence of the model to its input and may be viewed as an innovative approach to tackle Gibbs-induced phenomenon [19]. The method is in general more accurate than the classical approach with the same level of approximation and at no significant additional computational or memory cost, since it is deployed in a *post-processing* stage. Some other recent *solution-adaptive* techniques may be more accurate than i-gPC but they follow a different strategy and construct their computational grid in a sequential fashion [21, 80].

The i-gPC approach is gPC-based, therefore it inherits *de facto* its well-known curse of dimensionality. As a result it should not be used as a remedy to gPC facing the dimensionality problem. In practice, it works well for a moderate number of random dimensions (cf. example with 5 dimensions in [58]) as long as the system response is sufficiently well sampled to capture most of its relevant features. Moreover, i-gPC may benefit from recent sparse grid integration techniques developed for stochastic spectral projection method in order to reduce the curse-of-dimensionality associated with the conventional tensor-product integration rules [6, 39].

The i-gPC is an iterative method that consists in a first step and the iteration of the same procedure. The first step corresponds to the application of the standard gPC framework described in the previous section. Suppose $\theta \in \mathbb{R}^d$ denotes our random input, i.e., a

random vector with n independent random variable components. We suppose its probability measure $d\mathbb{P}^\theta$ — a product of the probability measure of its independent components — is known together with its $L^2(\Theta, \mathcal{B}, \mathbb{P})$ -corresponding orthonormal polynomial chaos basis $(\phi_\alpha^\theta)_{\alpha \in \mathbb{N}^d}$. We then wish to approximate a random variable $Y = u(\theta)$, where u is a (possibly nonlinear) transformation θ^\dagger . In the context of the Galerkin-based spectral projection formalism, this may be done by introducing a N points quadrature rule $(\theta_l, w_l)_{l \in \{1, \dots, N\}}$ in order to compute the gPC coefficients of Y in the P -truncated basis $(\phi_k^\theta)_{k \in \{0, \dots, P\}}$

$$y_k^\theta = \mathbb{E}[u(\theta)\phi_k^\theta(\theta)] \approx \sum_{l=1}^N \omega_l u(\theta_l) \phi_k^\theta(\theta_l), \quad \forall k \in \{0, \dots, P\},$$

where the multi-index has been changed to P for ease of notation.

The approximation $Y \approx Y_\theta^P(\theta) = \sum_{k=0}^P y_k^\theta \phi_k^\theta(\theta)$ converges with P in the L^2 -sense when the $(y_k^\theta)_{k \in \{0, \dots, P\}}$ are accurately estimated and the basis dimensionality P sufficiently large for the problem at hand. Note that $P \equiv P(Q, d)$ depends on the truncation order Q of the representation in each dimensions. In the following, the dependence of P with respect to Q and d is recalled only when necessary.

In the second step of i-gPC, which defines the iterative procedure, we build an approximation basis orthonormal with respect to the random variable $Z \equiv Y_\theta^P(\theta)$. We denote $(\phi_k^Z)_{k \in \mathbb{N}}$ the new basis with $d\mathcal{P}^Z$ the associated probability measure[‡]. Based on moment theory [26, 48], several algorithms are available, using Christoffel's formulae, Chebyshev algorithm, or the modified Chebyshev algorithm (used in this paper), see [11] for more details. We introduce the i^{th} statistical moment $(s_i^Z)_{i \in \mathbb{N}}$ defined as:

$$s_i^Z = \mathbb{E}[Z^i] = \int x^i d\mathcal{P}^Z(x) \approx \sum_{l=1}^N \omega_l \left(Y_\theta^P(\theta_l) \right)^i, \quad \forall i \in \mathbb{N}, \quad (3.3)$$

and approximated via the former quadrature rule.

We now seek the development of $Y = u(\theta)$ in the newly adapted approximation basis $(\phi_k^Z)_{k \in \mathbb{N}}$:

$$\begin{aligned} y_k^Z &= \mathbb{E} \left[u(F_\theta^{-1}(F_Z(Z))) \phi_k^Z(Z) \right] \\ &= \int u(x) \phi_k^Z \left(\sum_{l=0}^P y_l^\theta \phi_l^\theta(\theta) \right) d\mathbb{P}^\theta(x) \\ &\approx \sum_{l=1}^N \omega_l u(\theta_l) \phi_k^Z \left(\sum_{t=0}^P y_t^\theta \phi_t^\theta(\theta_l) \right), \quad \forall k \in \{0, \dots, R\}, \end{aligned} \quad (3.4)$$

where F_θ and F_Z denote the cumulative density function (cdf) of respectively θ and Z . Notice that the approximation reuses the N available points $(u(\theta_l), w_l)_{l \in \{1, \dots, N\}}$ and does not need additional model simulations.

[†]Transformation in a broad sense i.e., Y can be the output of a code etc.

[‡]Let us note that the dimensionality of this univariate basis is much lower than the dimensionality of the multivariate basis $(\phi_\alpha^\theta)_{\alpha \in \mathbb{N}^d}$.

The dimension R is kept constant through the entire iterative scheme and chosen close to the polynomial order value Q at the initial step, i.e., $R \sim Q$. This choice is central for multi-dimensional problems when $n > 1$, because it implies that $R \ll P$.

The following steps of the approach consists in successive iterations of the second step. If we call $Z^{m+1} \equiv Y_{Z^m}^Q(Z^m)$, the $(m+1)$ -th approximation of Y in the Q -truncated basis $(\phi_k^{Z^m})_{k \in \mathbb{N}}$ and let $\theta \equiv Z^0$ be the initial input random variable and $Y = u(\theta) = u(Z^0)$, then we can prove (assuming *exact* integration of Eqs. (3.3) and (3.4)) [58]:

$$\|Y - Y_{Z^{m+1}}^Q(Z^{m+1})\|_{L^2} \leq \|Y - Y_{Z^m}^Q(Z^m)\|_{L^2}, \quad (3.5)$$

indicating that successive iterations ensure better approximations.

Practical applications of the method, in particular in the context of computationally expensive u functional evaluation, suggest that the accuracy of the representation will be governed by the accuracy of the numerical integrations involved in the scheme. A more thorough analysis of the interplay of quadrature/aliasing and truncation errors as well as possible improvement of the method are assessed in [53].

4 Convergence of the posterior distribution

A relevant question relates to the impact of a mean square converging forward model onto the accuracy of the inferred posterior distribution. Marzouk et al. [43] have proved that if the approximate forward model converges to the true model in the L^2 sense, then the approximate posterior probability converges to the true posterior probability in the sense of the Kullback-Leibler (KL) divergence. This may be summarized as the following proposition:

Proposition 4.1. Let $\{u_i = u(x_i, \cdot)\}_{i \in \{1, \dots, N\}}$ be a set of N samples of the exact forward model and $\tilde{u}_{n,i}$ its approximate model built with $n < N$ evaluations of the exact forward model. We assume that the measure error is Gaussian, centered, with known standard error. Let π_{pr} be the prior on θ on Θ . Let π_{post} be the exact posterior and $\tilde{\pi}_{\text{post}}^n$ the approximate posterior distributions. Then, there exists a real strictly positive constant C such as

$$\boxed{D_{\text{KL}}(\pi_{\text{post}} \| \tilde{\pi}_{\text{post}}^n) \leq C \sum_{i=1}^N \|\tilde{u}_{n,i} - u_i\|_{L^2(\Theta)}. \quad (4.1)}$$

In their study, it was shown that the rate of convergence of the approximate posterior was higher than the one of the approximate forward model. In this section, we propose to prove the following proposition (cf. Proposition 4.2) which ensures that if the approximate model converges in the L^2 sense, then the posterior converges in the KL sense, and at least *two* times faster.

Proposition 4.2. Let, for $i \in \{1, \dots, N\}$, $u_i = u(x_i, \cdot)$ be the exact forward model and $\tilde{u}_{n,i}$ its approximate model built with n evaluations of the exact forward model. We assume that

the measure error is Gaussian, centered, with known standard error. We assume that the prior is *uniform* on Θ . Let π_{post} be the exact posterior and $\tilde{\pi}_{\text{post}}^n$ the approximate posterior. Then, there exists a real strictly positive constant C such as

$$\boxed{D_{\text{KL}}(\pi_{\text{post}} \parallel \tilde{\pi}_{\text{post}}^n) \leq C \left\{ \sum_{i=1}^N \|\tilde{u}_{n,i} - u_i\|_{L^2(\Theta)} \right\}^2.} \quad (4.2)$$

In order to carry on with the proof, we introduce some useful definitions and theorems.

4.1 Few prior definitions and theorems

In probability and information theory, the Kullback-Leibler divergence (D_{KL}) [30] quantifies the dissimilarity between two probability measures. This particular f -divergence [35] is not a distance because it is not symmetric and does not respect the Minkowski's inequality. D_{KL} is null if and only if the two distributions are identical.

Definition 4.1 (Kullback-Leibler divergence). Let Θ be a set included in \mathbb{R}^d and (p, q) two probability density functions on Θ such as almost everywhere $q(\theta) > 0$ ($\mathbb{P}(q(\theta) > 0) = 1$). The KL divergence between p and q is defined as

$$D_{\text{KL}}(p \parallel q) = \int_{\Theta} p(\theta) \log \left(\frac{p(\theta)}{q(\theta)} \right) d\theta. \quad (4.3)$$

D_{KL} may be numerically approximated via Monte-Carlo integration using n uniformly distributed samples θ_i on Θ .

In the following, we also need to introduce a symmetric version of the D_{KL} between p and q , also called the Jeffrey's divergence [25], defined as

$$\begin{aligned} D_{\text{KL}}^s(p \parallel q) &= D_{\text{KL}}(p \parallel q) + D_{\text{KL}}(q \parallel p) \\ &= \int_{\Theta} \{p(\theta) - q(\theta)\} \log \left(\frac{p(\theta)}{q(\theta)} \right) d\theta. \end{aligned} \quad (4.4)$$

Moreover, we will need to resort to the notion of variation between two probability measures. The total variation (TV) is a distance between two probability measures and is defined as follows.

Definition 4.2 (Total variation). Let Θ be a set in \mathbb{R}^d with the Borelian σ -algebra \mathcal{B} and (p, q) two probability measures on Θ . The total variation between p and q is

$$\text{TV}(p, q) = \sup_{A \in \mathcal{B}} |p(A) - q(A)|. \quad (4.5)$$

Finally, the Pinsker's inequality [52] relates TV and D_{KL} . It states that the total variation between two probability distributions is bounded by the square root of their KL divergence.

Theorem 4.1 (Pinsker's inequality). *Let Θ be a set with the σ -algebra \mathcal{B} . Let (p, q) be two probability distributions on Θ . Then,*

$$\boxed{\text{TV}(p, q) \leq \sqrt{\frac{1}{2} D_{\text{KL}}(p \| q)}}. \quad (4.6)$$

For the proof of Pinsker's inequality, see [52]. Taking the Borelian σ -algebra, this theorem has the following corollary.

Corollary 4.1 Let Θ be a set included in \mathbb{R}^d with the Borel σ -algebra \mathcal{B} and (p, q) two probability distributions on Θ . Then,

$$\sup_{\theta \in \Theta} |p(\theta) - q(\theta)| \leq \sqrt{\frac{1}{2} D_{\text{KL}}(p \| q)}. \quad (4.7)$$

Proof. For $\theta \in \Theta$, the singleton $\{\theta\}$ is in the σ -algebra \mathcal{B} . Then, the set of the singletons is included in \mathcal{B} . Then, applying Pinsker's inequality to this set (Theorem 4.1), leads to the result. ■

Now that we have the tools for the study of the convergence of the approximate posterior, we prove the main theoretical result in this paper (Eq. (4.2)).

4.2 Proof of Proposition 4.2

In order to prove the inequality (4.2), we introduce useful lemmas.

Lemma 4.1. *The function $x \mapsto e^{-x}$ is uniformly Lipschitz on $[0, +\infty]$. That is to say, there exists a constant Λ strictly positive such as for all $x \geq 0$ and for all $y \geq 0$: $|e^{-x} - e^{-y}| \leq \Lambda |x - y|$.*

Lemma 4.2. *With the notations of the previous sections, there exists a strictly positive real constant C_1 such as*

$$\boxed{|\gamma_n - \gamma| \leq C_1 \sum_{i=1}^N \|\tilde{u}_{n,i} - u_i\|_{L^2(\Theta)}}. \quad (4.8)$$

Proof. To begin with, for each point measure i , the approximate model $\tilde{u}_{n,i}$ converges in norm L^2 toward u_i . Consequently, $(\tilde{u}_{n,i})_{n \in \mathbb{R}}$ is bounded in norm L^2

$$\forall i \in \{1, \dots, N\} : \|\tilde{u}_{n,i}\|_{L^2(\Theta)} \leq \max_{1 \leq i \leq N} \sup_{n \in \mathbb{R}} \|\tilde{u}_{n,i}\|_{L^2(\Theta)} = C_N. \quad (4.9)$$

Then, by definition of γ_n and γ (2.5)

$$\gamma_n - \gamma = \int_{\Theta} \pi_{\text{pr}}(\theta) \left[\prod_{i=1}^N \pi_{\varepsilon}(\tilde{u}_{n,i}(\theta) - m_i) - \prod_{i=1}^N \pi_{\varepsilon}(u_i(\theta) - m_i) \right] d\theta. \quad (4.10)$$

Using the hypothesis of a Gaussian measure error,

$$|\gamma_n - \gamma| \leq \int_{\Theta} \pi_{\text{pr}}(\theta) \left| \exp \left[-\frac{1}{2\sigma^2} \sum_{i=1}^N (\tilde{u}_{n,i}(\theta) - m_i)^2 \right] - \exp \left[-\frac{1}{2\sigma^2} \sum_{i=1}^N (u_i(\theta) - m_i)^2 \right] \right| d\theta. \quad (4.11)$$

Using Lemma 4.1,

$$|\gamma_n - \gamma| \leq \frac{\Lambda}{2\sigma^2} \int_{\Theta} \pi_{\text{pr}}(\theta) \left| \sum_{i=1}^N (u_i(\theta) - m_i)^2 - (\tilde{u}_{n,i}(\theta) - m_i)^2 \right| d\theta, \quad (4.12a)$$

$$|\gamma_n - \gamma| \leq \frac{\Lambda}{2\sigma^2} \int_{\Theta} \pi_{\text{pr}}(\theta) \left| \sum_{i=1}^N (u_i(\theta) - \tilde{u}_{n,i}(\theta)) (u_i(\theta) + \tilde{u}_{n,i}(\theta) - 2m_i) \right| d\theta, \quad (4.12b)$$

$$|\gamma_n - \gamma| \leq \frac{\Lambda}{2\sigma^2} \sum_{i=1}^N \int_{\Theta} \pi_{\text{pr}}(\theta) |u_i(\theta) - \tilde{u}_{n,i}(\theta)| |u_i(\theta) + \tilde{u}_{n,i}(\theta) - 2m_i| d\theta. \quad (4.12c)$$

Applying Hölder's inequality for each integral in the sum,

$$|\gamma_n - \gamma| \leq \frac{\Lambda}{2\sigma^2} \sum_{i=1}^N \|u_i - \tilde{u}_{n,i}\|_{L^2(\Theta)} \|u_i + \tilde{u}_{n,i} - 2m_i\|_{L^2(\Theta)}. \quad (4.13)$$

By inequality (4.9),

$$|\gamma_n - \gamma| \leq (\max_i \|u_i\|_{L^2(\Theta)} + 2\max_i |m_i| + C_N) \frac{\Lambda}{2\sigma^2} \sum_{i=1}^N \|u_i - \tilde{u}_{n,i}\|_{L^2(\Theta)}. \quad (4.14)$$

Introducing

$$C_1 = (\max_i \|u_i\|_{L^2(\Theta)} + 2\max_i |m_i| + C_N) \frac{\Lambda}{2\sigma^2}, \quad (4.15)$$

we obtain

$$|\gamma_n - \gamma| \leq C_1 \sum_{i=1}^N \|u_i - \tilde{u}_{n,i}\|_{L^2(\Theta)}. \quad (4.16)$$

So, we complete the proof. ■

Lemma 4.3. Let $(a_k)_{k \in \mathbb{R}}$ and $(b_k)_{k \in \mathbb{R}}$ be two real strictly positive sequences and $a \in \mathbb{R}_+^*$ such as $\forall k \in \mathbb{R}$

$$|a_k - a| \leq b_k \quad \text{and} \quad \lim_{k \rightarrow +\infty} b_k = 0. \quad (4.17)$$

Then, there exists a real constant $M > 0$ such as $\forall k \in \mathbb{R}$

$$\left| \log \left(\frac{a_k}{a} \right) \right| \leq M b_k. \quad (4.18)$$

Proof. By hypothesis,

$$\forall n \in \mathbb{R}: |a_k - a| \leq b_k, \quad (4.19)$$

which leads to,

$$\forall k \in \mathbb{R}: 1 - \frac{b_k}{a} \leq \frac{a_k}{a} \leq 1 + \frac{b_k}{a}. \quad (4.20)$$

We notice that for a given $k_0 \in \mathbb{N}$, $1 - b_k/a > 0$. Therefore,

$$\forall k > k_0: \log\left(1 - \frac{b_k}{a}\right) \leq \log\left(\frac{a_k}{a}\right) \leq \log\left(1 + \frac{b_k}{a}\right) \leq \frac{b_k}{a}, \quad (4.21)$$

and

$$\forall k > k_0: \left| \log\left(\frac{a_k}{a}\right) \right| \leq \max\left\{-\log\left(1 - \frac{b_k}{a}\right), \frac{b_k}{a}\right\}. \quad (4.22)$$

The leading term in the right hand side is b_k/a when $k \rightarrow +\infty$. Then, $|\log(a_k/a)|$ is of order $\mathcal{O}(b_k)$. Then, there exists a constant C such that $\forall k > k_0: |\log(a_k/a)| \leq Cb_k$.

Finally, setting

$$M = \max\left\{C, \frac{|\log(\frac{a_0}{a})|}{b_0}, \dots, \frac{|\log(\frac{a_{k_0})}{a})|}{b_{k_0}}\right\},$$

we conclude that

$$\forall k \in \mathbb{R}: \left| \log\left(\frac{a_k}{a}\right) \right| \leq Mb_k, \quad (4.23)$$

which ends the proof. ■

Lemma 4.4. *There exists a constant $C_2 > 0$ such as:*

$$\boxed{\left| \log\left(\frac{\gamma_n}{\gamma}\right) \right| \leq C_2 \sum_{i=1}^N \|\tilde{u}_{n,i} - u_i\|_{L^2(\Theta)}. \quad (4.24)}$$

Proof. We apply the Lemmas 4.3 and 4.2 with

$$a_n = \gamma_n, \quad (4.25a)$$

$$b_n = \sum_{i=1}^N \|u_i - \tilde{u}_{n,i}\|_{L^2(\Theta)} \xrightarrow{n \rightarrow \infty} 0 \quad (\text{cf. Cameron Martin theorem [5]}). \quad (4.25b)$$

The lemma is proved. ■

Proof of the Proposition 4.2. First, we notice that the D_{KL} is smaller than Jeffrey's divergence

$$0 \leq D_{\text{KL}}(\pi_{\text{post}} \|\tilde{\pi}_{\text{post}}^n) \leq D_{\text{KL}}^s(\pi_{\text{post}} \|\tilde{\pi}_{\text{post}}^n). \quad (4.26)$$

We define

$$\Delta_n \equiv D_{\text{KL}}(\pi_{\text{post}} \|\tilde{\pi}_{\text{post}}^n). \quad (4.27)$$

From inequality (4.26), we have

$$\Delta_n \leq D_{\text{KL}}^s(\pi_{\text{post}} \parallel \tilde{\pi}_{\text{post}}^n). \quad (4.28)$$

Assuming that the prior is *uniform* ($1 = K_{\text{pr}} \pi_{\text{pr}}(\theta)$) and using the definition of Jeffrey's divergence, we rewrite

$$\Delta_n \leq K_{\text{pr}} \int_{\Theta} \left\{ \pi_{\text{post}}(\theta) - \tilde{\pi}_{\text{post}}^n(\theta) \right\} \log \left(\frac{\pi_{\text{post}}(\theta)}{\tilde{\pi}_{\text{post}}^n(\theta)} \right) \pi_{\text{pr}}(\theta) \, d\theta, \quad (4.29)$$

which may be bounded as follows

$$\Delta_n \leq K_{\text{pr}} \sup_{\theta \in \Theta} \left| \pi_{\text{post}}(\theta) - \tilde{\pi}_{\text{post}}^n(\theta) \right| \int_{\Theta} \left| \log \left(\frac{\pi_{\text{post}}(\theta)}{\tilde{\pi}_{\text{post}}^n(\theta)} \right) \right| \pi_{\text{pr}}(\theta) \, d\theta. \quad (4.30)$$

According to the Corollary 4.1 of Pinsker's inequality,

$$\Delta_n \leq K_{\text{pr}} \sqrt{\frac{1}{2} \Delta_n} \int_{\Theta} \left| \log \left(\frac{\pi_{\text{post}}(\theta)}{\tilde{\pi}_{\text{post}}^n(\theta)} \right) \right| \pi_{\text{pr}}(\theta) \, d\theta, \quad (4.31)$$

which leads to

$$\Delta_n^2 \leq K_{\text{pr}}^2 \frac{1}{2} \Delta_n \left\{ \int_{\Theta} \left| \log \left(\frac{\pi_{\text{post}}(\theta)}{\tilde{\pi}_{\text{post}}^n(\theta)} \right) \right| \pi_{\text{pr}}(\theta) \, d\theta \right\}^2 \quad (4.32)$$

and

$$\Delta_n \leq \frac{K_{\text{pr}}^2}{2} \left\{ \int_{\Theta} \left| \log \left(\frac{\pi_{\text{post}}(\theta)}{\tilde{\pi}_{\text{post}}^n(\theta)} \right) \right| \pi_{\text{pr}}(\theta) \, d\theta \right\}^2. \quad (4.33)$$

By introducing the likelihood function $l^{\mathcal{S}}$ and the approximate likelihood $l_n^{\mathcal{A}}$,

$$\Delta_n \leq \frac{K_{\text{pr}}^2}{2} \left\{ \log \left(\frac{\gamma_n}{\gamma} \right) + \int_{\Theta} \left| \log \left(\frac{l(\theta)}{l_n(\theta)} \right) \right| \pi_{\text{pr}}(\theta) \, d\theta \right\}^2, \quad (4.34a)$$

$$\Delta_n \leq \frac{K_{\text{pr}}^2}{4\sigma^2} \left\{ \log \left(\frac{\gamma_n}{\gamma} \right) + \int_{\Theta} \left| \sum_{i=1}^N (u_i(\theta) - m_i)^2 - (\tilde{u}_{n,i}(\theta) - m_i)^2 \right| \pi_{\text{pr}}(\theta) \, d\theta \right\}^2, \quad (4.34b)$$

$$\Delta_n \leq \frac{K_{\text{pr}}^2}{4\sigma^2} \left\{ \log \left(\frac{\gamma_n}{\gamma} \right) + \sum_{i=1}^N \int_{\Theta} |u_i(\theta) - \tilde{u}_{n,i}(\theta)| |u_i(\theta) + \tilde{u}_{n,i}(\theta) - 2m_i| \pi_{\text{pr}}(\theta) \, d\theta \right\}^2. \quad (4.34c)$$

Applying Hölder's inequality on each integral in the sum, we have

$$\Delta_n \leq \frac{K_{\text{pr}}^2}{4\sigma^2} \left\{ \log \left(\frac{\gamma_n}{\gamma} \right) + \sum_{i=1}^N \|u_i - \tilde{u}_{n,i}\|_{L^2(\Theta)} \|u_i + \tilde{u}_{n,i} - 2m_i\|_{L^2(\Theta)} \right\}^2. \quad (4.35)$$

$\mathcal{S}l = \prod_{i=1}^N \pi_{\varepsilon}(u_i(\theta) - m_i).$

$\mathcal{A}l_n = \prod_{i=1}^N \pi_{\varepsilon}(\tilde{u}_{n,i}(\theta) - m_i).$

By the Lemma 4.2,

$$\Delta_n \leq \frac{K_{\text{pr}}^2}{4\sigma^2} \left\{ C_2 \sum_{i=1}^N \|u_i - \tilde{u}_{n,i}\|_{L^2(\Theta)} + \sum_{i=1}^N \|u_i - \tilde{u}_{n,i}\|_{L^2(\Theta)} \|u_i + \tilde{u}_{n,i} - 2m_i\|_{L^2(\Theta)} \right\}^2. \quad (4.36)$$

We introduce C_3 as

$$C_3 \equiv \left(\max_i \|u_i\|_{L^2(\Theta)} + 2\max_i |m_i| + \sup_{n,i} \|\tilde{u}_{n,i}\|_{L^2(\Theta)} \right), \quad (4.37)$$

which exists given that all the u_i are in L^2 , that we have a finite number of measures and that all the $\tilde{u}_{n,i}$ converge in L^2 .

Then,

$$\Delta_n \leq \frac{K_{\text{pr}}^2}{4\sigma^2} \left\{ C_2 \sum_{i=1}^N \|u_i - \tilde{u}_{n,i}\|_{L^2(\Theta)} + C_3 \sum_{i=1}^N \|u_i - \tilde{u}_{n,i}\|_{L^2(\Theta)} \right\}^2. \quad (4.38)$$

Finally, introducing

$$C \equiv \frac{K_{\text{pr}}^2}{4\sigma^2} (C_2 + C_3)^2,$$

we conclude the proof by:

$$\Delta_n \leq C \left\{ \sum_{i=1}^N \|u_i - \tilde{u}_{n,i}\|_{L^2(\Theta)} \right\}^2. \quad (4.39)$$

Thus, we complete the proof of Proposition 4.2. \square

The inequality (4.1) ensures that, if we have a method to build approximate models that converge in the L^2 -sense (e.g., Polynomial Chaos or the iterative version of gPC), then the posterior converges in the KL sense. Moreover, in case of a *uniform* prior, the inequality (4.2) tells us that this convergence is twice faster.

5 Numerical comparisons

In this section, we demonstrate the predicted convergence rates of the posterior density function obtained by Bayesian inference for inverse problems of varying smoothness. For strongly nonlinear or discontinuous system response, we make use of our new representation of the forward model that is *adaptively* approximated by an iterative generalized Polynomial Chaos-based representation. The numerical approximations and predicted convergence rates of the former approach are compared to the new iterative numerical method.

This work is motivated by hydrodynamic application and the understanding of fluids interfaces for example for the study of Rychtmyer-Meshkov and Rayleigh-Taylor instabilities. As a consequence, the present test-cases are all nonlinear and, except the first one, inspired from hydrodynamic problem. Moreover, our adaptive approach was originally developed for dealing with the discontinuous cases but it is possible to apply our approach to other problems.

5.1 Step function

In this subsection we revisit one of the benchmarks first introduced in the paper by Marzouk and Xiu [40] and involving a discontinuity. The inverse problem involves a step function-like forward model that may be interpreted as follows: let us consider a one-dimensional linear advection problem, defined on $\Theta = [-1; 1]$, with a discontinuous initial condition $u_0(x)$ representative of a shock-dominated solution:

$$u_0(x) = \mathbb{I}_{[x < 0]}(x) = \begin{cases} 0, & \text{if } x \leq 0, \\ 1, & \text{elsewhere.} \end{cases} \quad (5.1)$$

Later on, the shock will be advected in time and the solution may be written as $u(x, t) = u_0(x - vt)$, for $t > 0$. The goal is to infer on the shock speed $v (= \theta)$ based on a single observation m , from a detector placed at $(x = 0, t = 1)$ with finite accuracy. The measure $m = u(v_{\text{true}}) + \eta$ is artificially perturbed by a Gaussian noise $\eta \sim \mathcal{N}(0, \nu^2)$ with a standard deviation $\nu = 0.1$. We assume that the measure error law π_ε considered in our Bayesian formalism is known, chosen as $\varepsilon \sim \eta \sim \mathcal{N}(0, \nu^2)$. We assume that we have no particular initial knowledge about the shock speed or its direction, so we model it as a *uniform* prior distribution over the entire domain range $[-1; 1]$. We choose $v_{\text{true}} = 0.2$ as the true value for the shock speed.

Despite its simplicity (exact solution is available), this academic problem is numerically difficult mainly because of the discontinuity.

The numerical methods described in previous sections are applied to this problem. Figs. 4(a) and 4(b) show the results of the inverse problem for gPC and i-gPC approximate representations compared to the exact solution. Fig. 4(a) shows the approximation of the forward model and Fig. 4(b) shows the posterior probability distribution functions of v . A Legendre polynomial basis approximation of order $P = 9$ is chosen together with numerical quadrature of Clenshaw-Curtis (CC) type of level $l = 8$, with $2^{l-1} + 1 = 129$ quadrature points.

The gPC-based Bayesian inference performs in this case very poorly as the oscillations of the approximate forward model are inherited and amplified by the nonlinearity of the ε Gaussian density. However, it is very clear that the i-gPC approach avoids the spurious oscillations of the gPC representation which artificially emphasizes certain values of $v > 0$ and assigns very low probability of occurrence to values of v lower than $v_{\text{true}} = 0.2$, due to the oscillations of \tilde{u}_n^{gPC} .

For high level of integration accuracy, the study may be reiterated for different choices of truncation order P . In the following, we perform a convergence analysis of the quantities defined as:

$$\pi_{\text{post}}(v) \propto \pi_{\text{pr}}(v) \pi_\varepsilon(u(v) - m), \quad (5.2a)$$

$$\pi_{\text{post}}^{n, \text{gPC}}(v) \propto \pi_{\text{pr}}(v) \pi_\varepsilon(\tilde{u}_n^{\text{gPC}}(v) - m), \quad (5.2b)$$

$$\pi_{\text{post}}^{n, \text{i-gPC}}(v) \propto \pi_{\text{pr}}(v) \pi_\varepsilon(\tilde{u}_n^{\text{i-gPC}}(v) - m). \quad (5.2c)$$

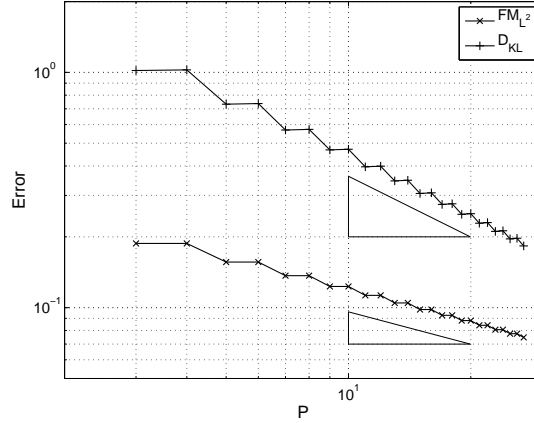


Figure 1: Step function test case: convergence study with respect to gPC truncation order P of the forward model approximation error $\|\tilde{u}_{n,i} - u_i\|_{L^2(\Theta)}$ (FM_{L^2}) and the posterior density Kullback-Leibler divergence $D_{KL}(\pi_{\text{post}} \|\tilde{\pi}_{\text{post}}^n)$ (D_{KL}).

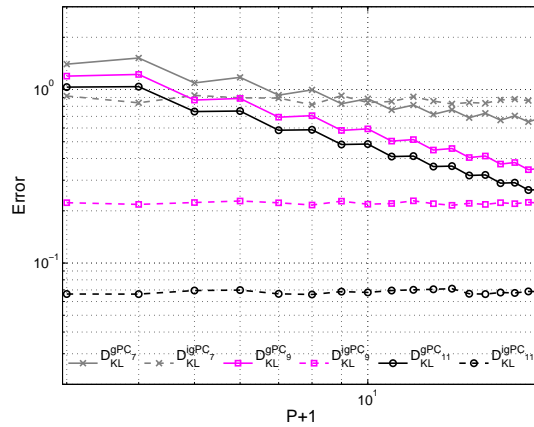


Figure 2: Step function test case: comparison between posterior density Kullback-Leibler divergence $D_{KL}(\pi_{\text{post}} \|\tilde{\pi}_{\text{post}}^n)$ obtained from gPC (D_{KL}^{gPC}) and i-gPC ($D_{KL}^{\text{i-gPC}}$) forward model approximations for different quadrature levels.

Fig. 1 validates the theoretical results presented in Section 4. It shows the convergence rates numerically evaluated for the gPC representation in a log-log plot. The bottom curve shows the *algebraic* convergence of the model approximation $\|\tilde{u}_{n,i} - u_i\|_{L^2(\Theta)}$ (FM_{L^2}) while the top confirms that the posterior density Kullback-Leibler divergence $D_{KL}(\pi_{\text{post}} \|\tilde{\pi}_{\text{post}}^n)$ (D_{KL}) decreases twice as fast, as predicted by the theory (cf. Proposition 4.2) and also observed for stochastic collocation approximation [40]. The study is also performed for the i-gPC representation with the same dimensionality and underlying quadrature. This time the Kullback-Leibler divergence is much lower, cf. Fig. 2, which indicates that the posterior density is more accurate. The truncation order P does not

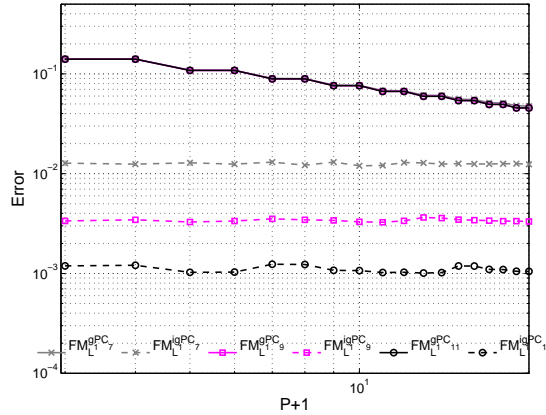


Figure 3: Step function test case: comparison between gPC ($FM_{L_1}^{gPC}$) and i-gPC ($FM_{L_1}^{igPC}$) forward model errors in L^1 -norm for different quadrature levels.

seem to be the limiting factor while the effect of the aliasing error related to the quadrature accuracy is in this case dominant. This is confirmed when we look at the errors of the approximated gPC and i-gPC forward models in L^1 -norm in the convergence study with respect to the truncature order P (abscissae) and the quadrature accuracy (colors of the curves), displayed in Fig. 3. We notice in this case that the accuracy of the i-gPC model is bounded by the maximum resolution level between two neighbor points in the quadrature grid whereas the accuracy of gPC is bounded by the truncature order P independently of the quadrature accuracy. Therefore, a relevant question relates to the robustness of the method for less accurate numerical integration.

Figs. 4-5 show the results obtained for a Legendre polynomial basis approximation of order $P = 9$ and $P = 4$ with numerical quadrature of CC type of level 11 with 1023 quadrature points and with $l = 6$ with 33 quadrature points respectively. The i-gPC-based posterior estimation is very close to the exact solution. On Fig. 5, the number of functional evaluations and the polynomial order being lower, the projection error is higher, but remarkably i-gPC is still able to recover the uniform law of the true posterior, it captures the discontinuity better and avoids the apparition of oscillations.

It is interesting to assess the advantage of the i-gPC representation compared to other methods [38, 58]. Here, we revisit the straightforward but challenging example of the discontinuous step function treated in [58], but in the context of finite numerical integration, i.e., the forward model will only be evaluated a finite (moderate) number of times. The goal is to compare the accuracy of pseudo-spectral gPC, stochastic collocation [67], h -adaptive piecewise polynomial (also referred as Multi-Element-gPC [34, 73]) and i-gPC approximations. We refer the reader to [38] for other types of approximations/comparisons.

Stochastic collocation is based on an interpolation on Lagrange polynomials at the quadrature points. ME-gPC is an adaptive and sequential approach consisting in tracking

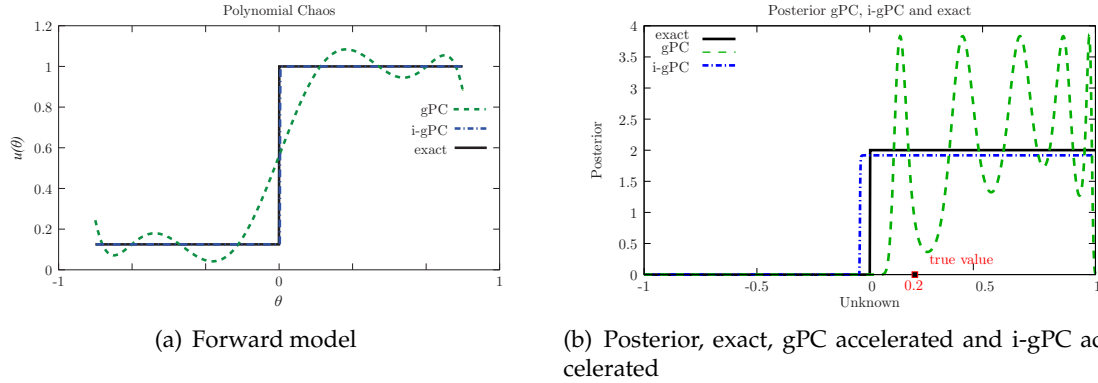


Figure 4: Exact forward model, gPC approximate model with a polynomial order $P=9$, i-gPC approximate model with a polynomial order $P=9$. i-gPC captures the discontinuities while gPC cannot.

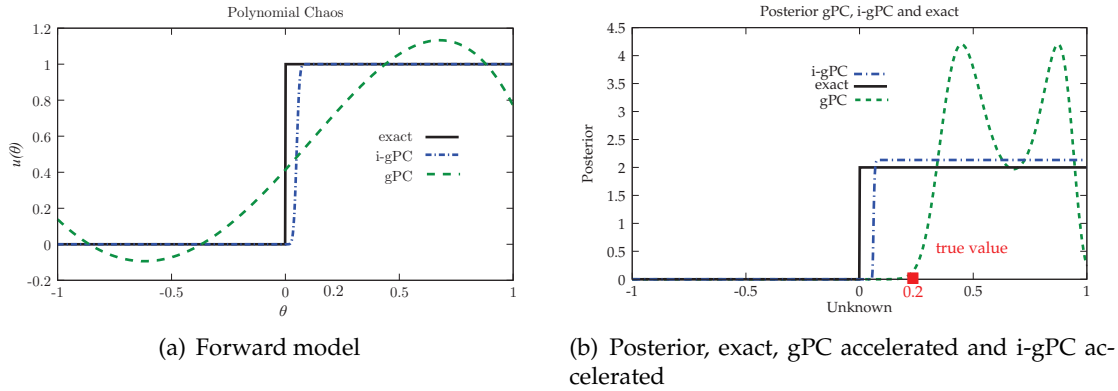


Figure 5: A realistic example: quadrature level $l=6$, $P=4$.

discontinuities in the stochastic space and decomposing it into several well-chosen (i.e., close to the discontinuity position) elements. To be fair, the comparison will be carried out on a common computational ground.

Let θ be a uniform random variable on $[-1;1]$ and u be the step function, equal to 1 on $[-1;-0.4]$ and 0 on $]-0.4;1]$. The random solution $Y = u(\theta)$ only takes two discrete values, i.e., the functional u maps a uniform distribution to a binomial distribution.

We choose to rely on a budget of 14 function samples for all methods: a *fixed* Gauss-Legendre (GL) grid is used except for the ME-gPC approximation where Clenshaw-Curtis (CC) grid points are *sequentially* introduced depending on the required elemental refinement decomposition. We test the gPC (Legendre-based chaos with truncature degree $P=3$ and $P=5$) and i-gPC representations making use of the previous gPC results together with a stochastic collocation (Lagrange-based nodal basis constructed on the GL points) and a ME-gPC approximation of first order Legendre-based chaos, i.e., $P=1$ and two boundary quadrature CC points in each element.

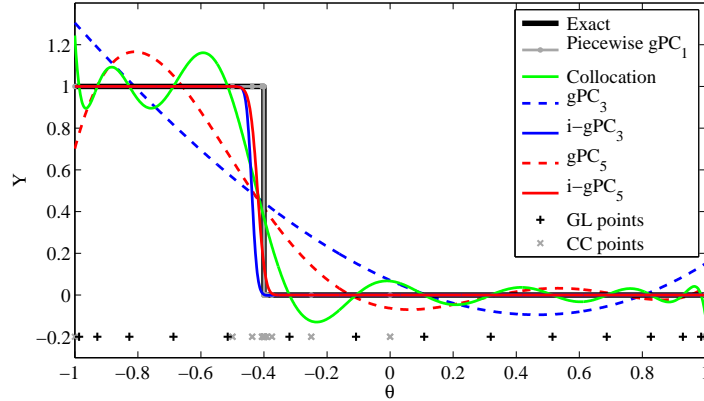


Figure 6: Step function test case: comparison between several types of approximation. Note: Gauss-Legendre (GL) 14 quadrature points are the training data for the stochastic collocation, gPC and i-gPC approximations and Clenshaw-Curtis (CC) 14 quadrature points are the sequential training data for the piecewise first-order gPC approximation.

Fig. 6 shows the results together with the analytical solution and the computational grids. gPC and collocation polynomial approximations strongly oscillate whereas ME-gPC and i-gPC approximations avoid Gibbs’ phenomenon: spurious (e.g., under- and overshoot) values are avoided which keeps the distribution of Y from artificially spreading. So the representations are in this sense more robust.

ME-gPC results are very accurate, cf. Table 1. i-gPC_{P=5} is also quite accurate, in particular in the L^1 norm which is the relevant one when dealing with systems of conservation law and discontinuous solutions. The i-gPC approach is also quite accurate at capturing the approximate location of the shock considering that the discontinuity is positioned in between two distant quadrature points.

Table 1: Comparison of accuracy of step function approximations (cf. Fig. 6) based on 14 function evaluations.

	L^1 -error	L^2 -error
Piecewise gPC $P=1$	9.0×10^{-5}	6.8×10^{-3}
gPC $P=3$	1.5×10^{-1}	2×10^{-1}
i-gPC $P=3$	1.9×10^{-2}	1.2×10^{-1}
gPC $P=5$	9.8×10^{-2}	1.6×10^{-1}
i-gPC $P=5$	1.1×10^{-2}	7.7×10^{-2}
Collocation	6.7×10^{-2}	1.1×10^{-1}

One may argue that ME-gPC (and other related adaptive approximations) do better than i-gPC for this type of problem. This is true but the approaches are completely different and therefore complementary: when i-gPC adapts the functional representation based on samplings from a given *arbitrary* and *fixed* grid, ME-gPC requires new samples in a *sequential* fashion based on some *ad hoc* heuristics. Moreover, i-gPC bears some ad-

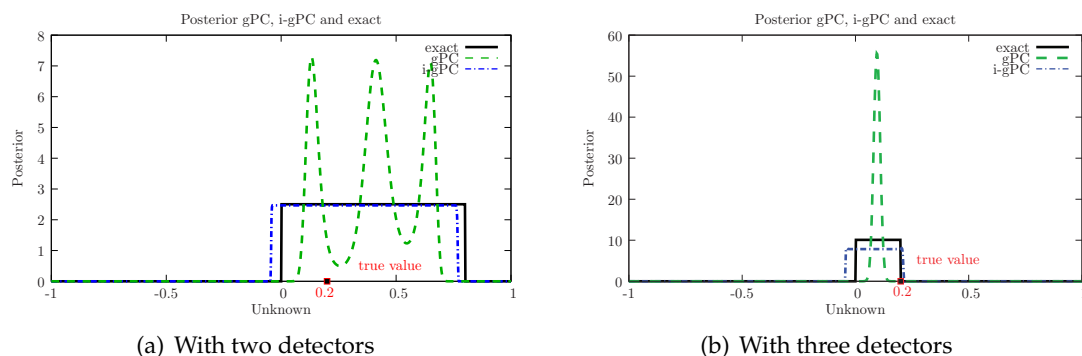


Figure 7: Same problem as in Fig. 4 but with two then three measurements at $x=0.1$, $t=1$ and $x=0.2$, $t=1$. Adding observations does not affect the uniformity of the posterior but allows narrowing its support.

vantages: when the output to represent is a random vector, as it is the case in a Bayesian framework as soon as there are several measurements, it relies on a single grid and does not need to adapt the computational grid to each quantity of interest/measurements; in terms of implementation, it may trivially take advantage of parallel computing which is not the case for sample-based sequential methods.

In the last paragraph of this section, we consider the same problem but we add a second then a third detector. The first detector was located at $x=0$ for $t=1$. We locate the second at $x=0.8$ and $t=1$ and the third at $x=0.2$ and $t=1$ and consider the posteriors obtained with the different methods. Fig. 7 shows the analytical posterior and the ones obtained with gPC and i-gPC. Let us first comment the analytical posterior: the increase in the number of observations does not affect the uniformity of the posterior, it only affects their supports. Indeed, with one measurement the posterior is uniform on $[0,1]$, with two it is uniform on $[0,0.8]$ and with three it is uniform on $[0,0.2]$. As the number of observations increases, the true value can be approached more precisely.

Note also that for such test-problem with several detectors, we were not able to apply ME-gPC in the same condition as the other methods: indeed, the sequentially built quadrature points of the algorithm are different for each observations increasing considerably the number of model calls with the number of measurements.

With a choice of a uniform prior, the posterior distribution is also uniform and non-informative about the true value of the parameter, at most predicting a narrower range of probability when multiplying observations. While this may foster several questions about the conditioning of inverse problems for systems with discontinuity, according to our study and others [4], the stochastic inverse problem framework remains adequate in this setup and shows that there is not one "most probable parameter" but several.

In conclusion, we can say that the global accuracy of the i-gPC representation, on this test problem, is constrained by the precision of the underlying numerical quadrature. A more thorough analysis of the interplay of quadrature/aliasing and truncation errors in this framework is presented in a different publication [53].

In the following section, we consider a nonlinear time-dependent problem with two and three stochastic dimensions demonstrating that the previous concepts are transposable in multi-dimensional stochastic context.

5.2 Inviscid Burgers equation

In this section, we show how the method behaves for nonlinear problems in higher stochastic dimensions. We consider the simplest hyperbolic nonlinear equation known as Burgers equation [9]:

$$\begin{cases} \partial_t u(x,t,\theta) + \partial_x \frac{u^2(x,t,\theta)}{2} = 0, \\ u_0(x,\theta) = u(x,0,\theta), \end{cases} \tag{5.3}$$

with a shock-dominated *uncertain* initial condition. Here we have two shocks whose locations are not precisely known within some bounded intervals.

$\theta = (\theta_0, \theta_1)$ are the unknown parameters related to the initial condition u_0 such that

$$u_0(x,\theta) = \begin{cases} u_1, & \text{if } x \leq x_0 + \sigma_0\theta_0, \\ u_2, & \text{if } x_0 + \sigma_0\theta_0 \leq x \leq x_1 + \sigma_1\theta_1, \\ u_3, & \text{if } x \geq x_1 + \sigma_1\theta_1. \end{cases} \tag{5.4}$$

For our practical applications, we choose the following parameters values: $u_1 = 2$, $u_2 = 1/2$, $u_3 = 0$, $x_0 = -0.5$, $x_1 = 0.5$, $\sigma_0 = 0.2$ and $\sigma_1 = 0.1$. As before, we build a test-case in which we know the true value of the parameter, here it is set to $\theta_{true} = (0.5, 0.5)$.

We consider a prior knowledge following a *uniform* distribution on $[-1;1]^2$. Fig. 8(a) shows several realizations of the initial condition corresponding to different values of θ . The system is then integrated in time. The first shock (left one on the figure) will move to the right faster than the second one until they merge.

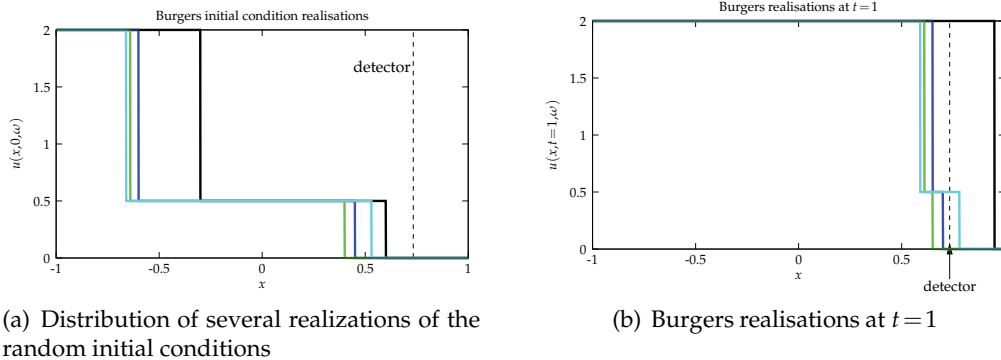


Figure 8: Several realizations of the initial condition and the solution at final time for the 2D Burgers problem.

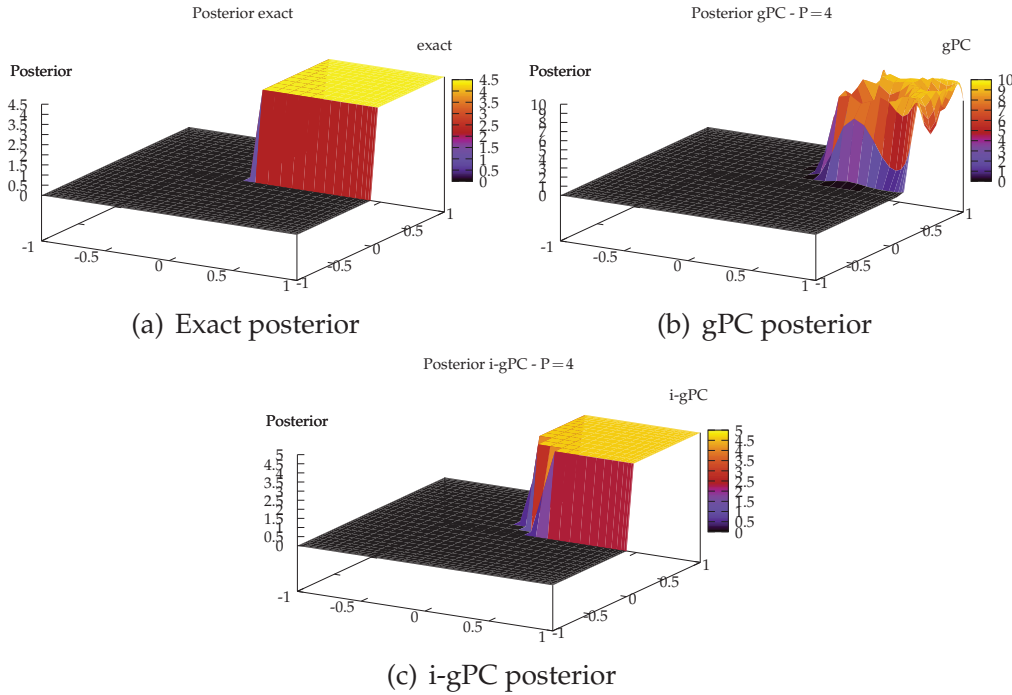


Figure 9: Exact posterior, gPC posterior and i-gPC posterior. $P=4$ and Clenshaw-Curtis quadrature level is 5. The gPC oscillations make us think that some parameters, among the positive one, are more probable than others. On the contrary, with i-gPC, we get an area of equi-probable parameters which is what says the exact posterior. Moreover, i-gPC gets better the discontinuities.

For this problem, an analytical solution is available and is given, at time t and at position x , by

$$u(x,t,\theta) = \begin{cases} u_1, & \text{if } x \leq x_0 + \sigma_0 \theta_0 + v_0 t, \\ u_2, & \text{if } x_0 + \sigma_0 \theta_0 + v_0 t < x \text{ and } x \leq x_1 + \sigma_1 \theta_1 + v_1 t, \\ u_3, & \text{if } x > x_1 + \sigma_1 \theta_1 + v_1 t. \end{cases} \quad (5.5)$$

$v_0 = (u_1 + u_2)/2$ and $v_1 = (u_2 + u_3)/2$. We suggest considering measurement at time $t = 1$ and at position $x = 0.75$. At this time and at this position, the response is a discrete random variable with three Dirac of different weights at u_0 , u_1 and u_2 . Fig. 8(b) shows the analytical solution in $x = 0.75$ and at $t = 1$ corresponding to different initial conditions (i.e., different values of the random parameter θ).

The approximate models gPC and i-gPC are constructed using a full two dimensional Clenshaw-Curtis grid of level 5 (289 runs of the forward model).

Fig. 9 presents the reference posterior, the posterior built from the gPC approximations at the measurement points and the posterior built with the i-gPC approximation at these same points. Note that the discontinuities are better captured with i-gPC than

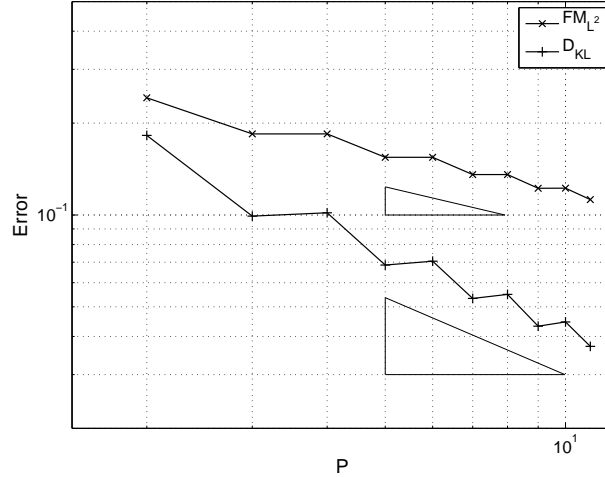


Figure 10: Inviscid Burgers test case: convergence study with respect to truncation order P of the forward model approximation error $\|\tilde{u}_{n,i} - u_i\|_{L^2(\Theta)}$ (FM_{L^2}) and the posterior density Kullback-Leibler divergence $D_{KL}(\pi_{\text{post}} \|\tilde{\pi}_{\text{post}}^n)$ (D_{KL}).

with gPC and the oscillations are reduced (see the different scales for the different approximations). The i-gPC approximation allows recovering the uniform distribution of the parameter in the high probability area whereas gPC tends to, first, miscalculate the support of the area of non zero probability: its support is smaller than expected and parameter values which are actually very probable are given probability zero. Suppose those parameters with high probability of occurrence correspond to defective situations, one would not want to miss them. Besides, the gPC approximations are very oscillating, giving birth to parameter values which seems to be more likely to occur whereas this is not the case: the i-gPC approximation allows recovering the uniform distribution.

Fig. 10 shows the gPC convergence of the approximate posterior in the sense of the Kullback-Leibler divergence and the convergence of the gPC approximate model in the sense of the L^2 error. The result is once again consistent with Proposition 4.2.

In this paragraph, we consider the same hyperbolic nonlinear equation as before, again with a shock-dominated *uncertain* initial condition, but this time we want to infer on the floors of the initial condition rather than on the shock positions.

In this section, $\theta = (\theta_1, \theta_2, \theta_3)$ are the unknown parameters related to the initial condition u_0 such that

$$u_0(x, \theta) = \begin{cases} \theta_1, & \text{if } x \leq x_0, \\ \theta_2, & \text{if } x_0 \leq x \leq x_1, \\ \theta_3, & \text{if } x \geq x_1. \end{cases} \quad (5.6)$$

For one realization of the initial conditions, we once again now the exact solution to

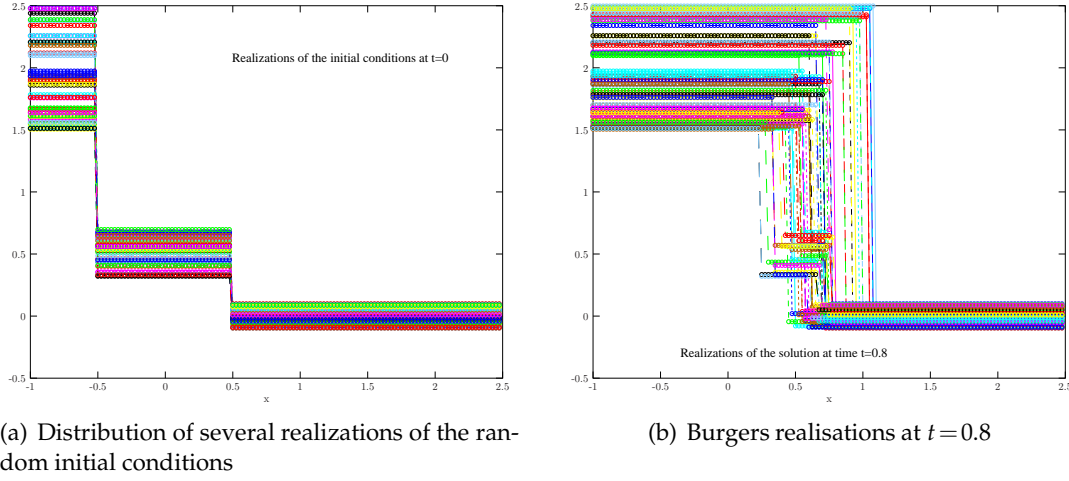


Figure 11: Several realizations of the initial condition and the solution at final time for the 3D Burgers problem.

this Burgers problem. At time t and at position x , the solution is given by

$$u(x,t,\theta) = \begin{cases} \text{if } t < t^* \begin{cases} \theta_1, & \text{if } x \leq x_0 + v_0 t, \\ \theta_2, & \text{if } x_0 + v_0 t < x \leq x_1 + v_1 t, \\ \theta_3, & \text{if } x > x_1 + v_1 t, \end{cases} \\ \text{if } t \geq t^* \begin{cases} \theta_1, & \text{if } x \leq x^* + v_2(t - t^*), \\ \theta_3, & \text{if } x > x^* + v_2(t - t^*), \end{cases} \end{cases} \quad (5.7)$$

where $v_0 = (\theta_1 + \theta_2)/2$, $v_1 = (\theta_2 + \theta_3)/2$ are the velocities of the two shocks for times $t < t^*$ with $t^* = 2(x_0 - x_1)/(\theta_3 - \theta_1)$ the time for which the fast shock reach the slow one. We denote by $x^* = x_0 + v_0 t^*$ the location where it occurs. Finally, $v_2 = (\theta_3 + \theta_1)/2$ is the shock velocity of the resulting shock when they collapse at (x^*, t^*) . This test-problem is interesting for example because we want to infer on the second floor which has a short time life $[0, t^*]$ depending on the realizations of θ , the positions of the detectors in our Bayesian context will have a great importance.

As before, we build a test-case in which we know the true value of the parameter, here it is set to $\theta^{true} = (\theta_1^{true} = 2, \theta_2^{true} = 0.5, \theta_3^{true} = 0)$ and the observations are once again artificially noised thanks to a gaussian distribution of zero mean and 0.1 standard deviation. The priors are taken uniform on $[1.8, 2.2] \times [0.3, 0.7] \times [-0.2, 0.2]$. Fig. 11 presents several realizations of the initial conditions (Fig. 11(a)) with the previous prior and of the solutions at time $t = 0.8$ (Fig. 11(b)). Initially, the shock positions are known but we want to infer on the floors of the initial condition, see Fig. 11(a). As time evolves, the left shock absorbs the right one at times depending on the vector of parameter $\theta = (\theta_1, \theta_2, \theta_3)$, see Fig. 11(b).

We use a level 4 Gauss-Legendre quadrature rule (17 points) with a polynomial expansion of order 6 in each stochastic direction.

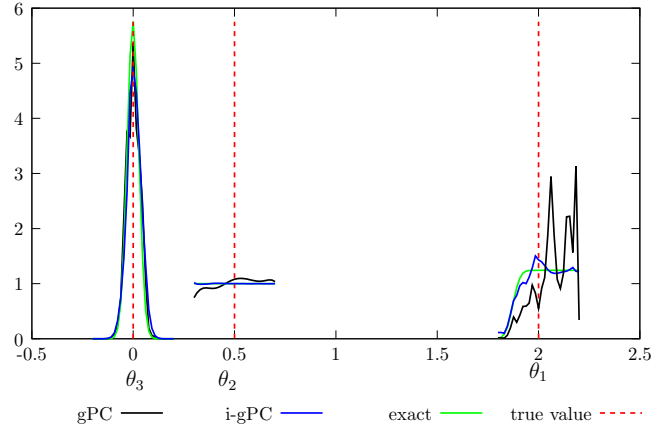


Figure 12: 3D Inviscid Burgers test case.

We considered a Bayesian problem with five observations at positions and times $x_1 = -0.75$, $t_1 = 0$, $x_2 = 0$, $t_2 = 0.5$ and $x_3 = 0.65$, $t_3 = 0.97$. Fig. 12 presents the results for the three marginals of the posterior obtained with the previous conditions. The vertical bars corresponds to the positions of the true values of the parameters, i.e., $\theta^{true} = (\theta_1^{true} = 2, \theta_2^{true} = 0.5, \theta_3^{true} = 0)$. Let us first consider the marginal with respect to θ_3 : Fig. 12 shows that gPC and i-gPC give equivalent results and allows inferring on the true values of parameter θ_3 . If we now consider the marginal with respect to θ_2 , we realize that the different measurements did not give information on the true value of θ_2 . Indeed, the analytical marginal is still uniform on $[0.3, 0.7]$. Note that for this marginal, the gPC approximated posterior presents spurious modes whereas i-gPC allows recovering the fact that the prior has not been updated by the measurements. Finally, the last marginal, with respect to θ_1 , is the most challenging for gPC and i-gPC but once again, i-gPC allows a gain in exactly the same conditions as gPC.

In the next section, we consider Euler system and compressible fluid dynamics and apply the above material to the main motivation of our work.

5.3 Euler system: stochastic Riemann problem

In this section, we consider an hydrodynamic compressible problem, where the initial location of the interface is uncertain. This test problem consists in a first step toward the study of uncertain interface position and mixing zone behaviours which play an important role in many applications. Our system is modeled by an Euler system:

$$\begin{cases} \partial_t \rho + \partial_x(\rho u) = 0, \\ \partial_t(\rho u) + \partial_x(\rho u^2 + p) = 0, \\ \partial_t(\rho e) + \partial_x(\rho u e + p u) = 0, \end{cases} \quad (5.8)$$

where the first equation corresponds to mass conservation, ρ is the mass density and u the velocity. The second equation corresponds to the conservation of impulsion, p is the pressure given by a perfect gas state equation. The last equation corresponds to total energy conservation, e is the specific total energy.

Let us consider a stochastic Riemann problem [62, 63, 68]. The problem initially consists of two constant states, a light fluid and a heavy fluid, separated by an interface whose abscissa is uncertain. The initial condition is given by

$$u(x,0,\theta) = \begin{cases} \rho(x,0,\theta) = \begin{cases} 1, & \text{if } x \leq \theta, \\ 0.125, & \text{elsewhere,} \end{cases} \\ \rho u(x,0,\theta) = 0, \\ \rho e(x,0,\theta) = \begin{cases} 2.5, & \text{if } x \leq \theta, \\ 0.25, & \text{elsewhere.} \end{cases} \end{cases} \quad (5.9)$$

θ corresponds to the initial abscissa interface. Its true value is set to 1. The prior on θ is an uniform distribution on $[0.95;1.05]$ and the error law for the measurement error and the noisy observations consists in a centered gaussian distribution of standard deviation $\sigma = 0.1$. We place a sensor at $x = 1.01$ (in real experiments, this sensor consists in a camera or equivalent sharp device, see [59, 70] for example), in the vicinity of the interface abscissa, and we consider 4 measurement times: $0, t_m/3, 2t_m/3$ and $t_m = 0.14$.

Fig. 13 presents three realisations of the uniform prior at different times together with the position of the detector for the measurements. As time passes, for one realisation, three waves are developing and propagating: a rarefaction fan (left) in the heavy fluid, a contact discontinuity (middle), interface between both fluids, and a shock (right) in the light fluid.

First, let us consider the different approximations at the different measurement points. In order to build the approximations, we rely on a non-intrusive Polynomial Chaos projection with a Gauss-Legendre integration grid of level 6 ($2^{6-1} + 1 = 33$ points) and level 8 ($2^{8-1} + 1 = 129$ points), and a polynomial order of $P = 7$.

Fig. 14 presents the analytical solution (reference) together with the gPC and i-gPC approximations at three measurement points ($t = 0, t = 0.046$ and $t = 0.14$). Let us first consider the dynamic of the flow and the analytical solutions. One can notice the different behaviour of the stochastic analytical solution at the measurement points with respect to time: the solution first consists in a discontinuity as the shock passes through the detector, see 14(a). Then, the detector captures both the contact discontinuity together with a part of the rarefaction fan, see 14(c). At the last measurement point, the detector only captures the rarefaction fan, see 14(b).

We now consider the behaviour of the different approximations at these measurement points. For the first measure, i-gPC allows recovering the discontinuous behaviour of the shock passing through the sensor whereas the gPC approximations oscillates (Fig. 14(a)). At measure two, in the vicinity of the rarefaction fan, both gPC and i-gPC gives satisfactory results (Fig. 14(c)). At measure three, where we observe both the contact discontinuity and the rarefaction fan, i-gPC allows an improvement especially in the vicinity of the

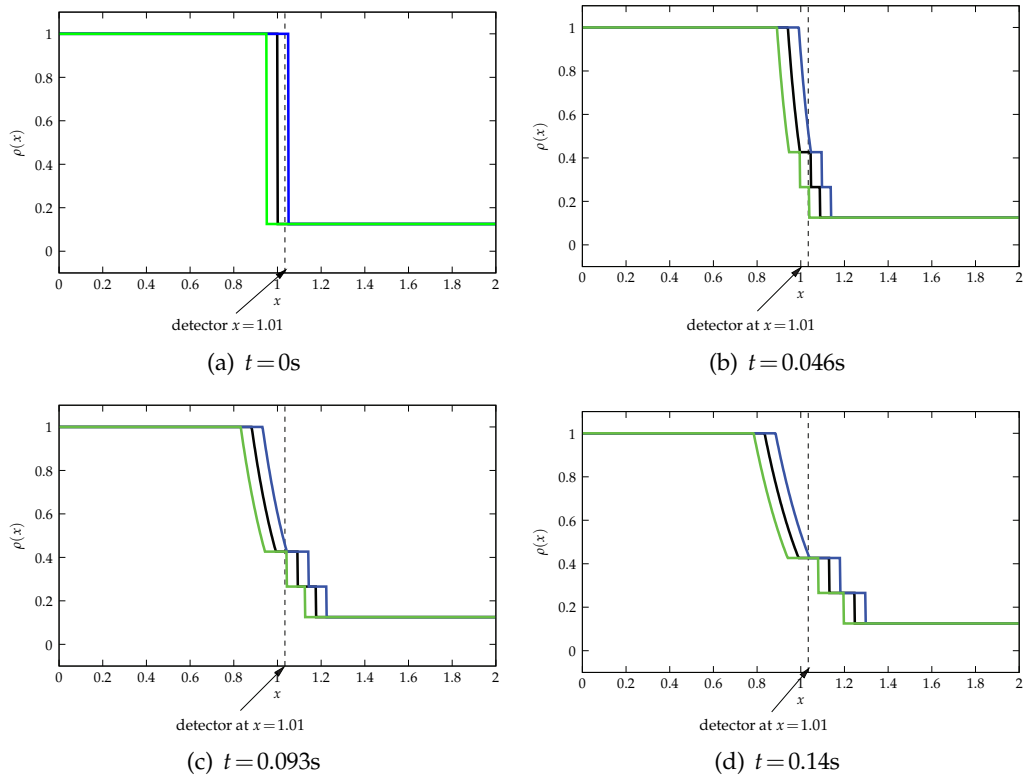
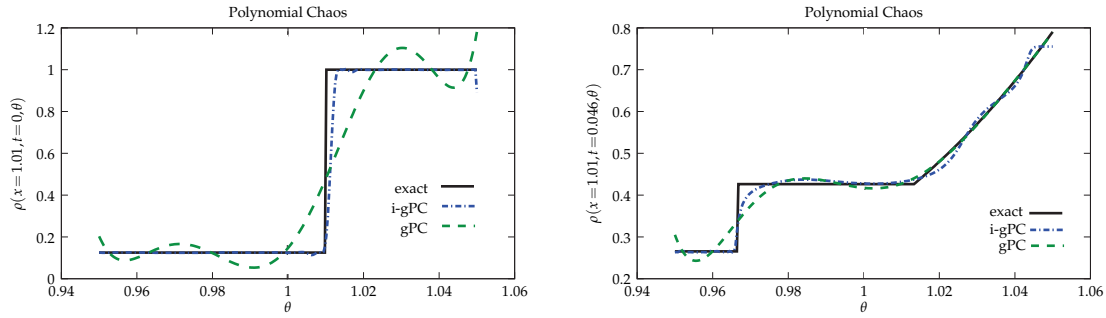


Figure 13: Density solution at four different times for different values of the initial interface abscissa: its mean value in black, its maximum value in blue and its minimum value in green.

discontinuity (Fig. 14(b)). In this sense, we consider i-gPC allows an adaptation of the basis with respect to the solution.

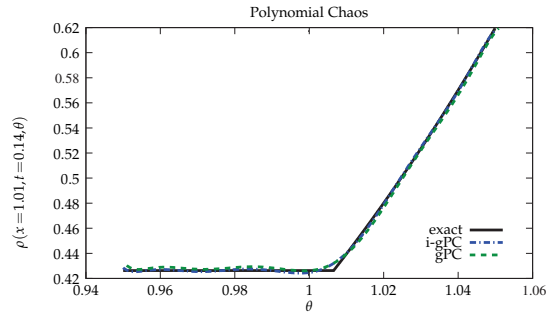
Figs. 15(a) and 15(b) present the reference posterior together with the gPC and i-gPC approximated ones. Once again, the analytical posterior density function exhibits a discontinuous behaviour. Once again, on this test problem, the use of gPC approximations can lead to bad interpretations: for example, according to the gPC accelerated posterior, the parameter value $\theta = 1.01$, where the sensor is located, is not considered as relevant whereas it is, see the reference posterior. On the contrary, the i-gPC accelerated posterior gives to this area the importance it deserves. Moreover, due to the oscillations of the gPC representation, the gPC accelerated posterior gives more weight to some points which is not the case with i-gPC.

Finally, Fig. 16 presents, on this same difficult problem, a convergence study in term of Kullback-Leibler divergence, L^1 norm and L^2 norm, of the gPC and i-gPC approximations with respect to both the number of integration points $2^{k-1} + 1$ and the polynomial order P . Let us first consider the gPC Kullback-Leibler convergence curves on the top of Fig. 16(a): as the number of integration points increases, the convergence speed decreases. This is due to the particular behaviour of gPC approximations in term of the



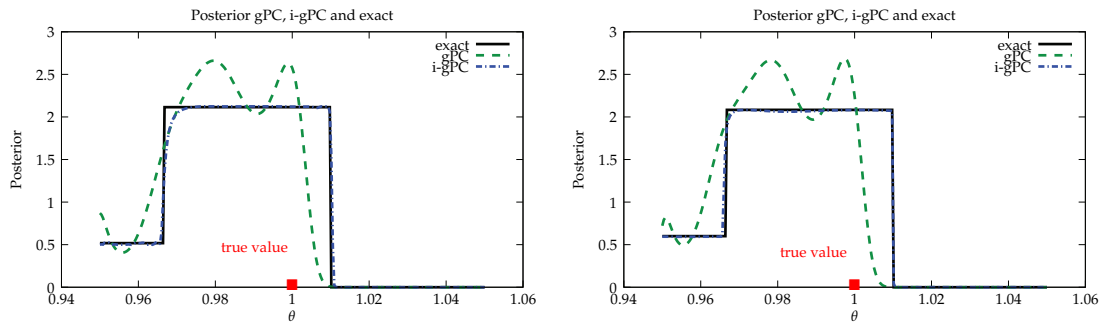
(a) Polynomial reconstruction at measure 1: shock wave, $t=0$

(b) Polynomial reconstruction at measure 3: shock and rarefaction waves, $t=0.046$



(c) Polynomial reconstruction at measure 2: rarefaction fan, $t=0.14$

Figure 14: Adaptation of the polynomial basis with i-gPC.



(a) Gauss-Legendre quadrature level is 6 (33 points). Polynomial order is 7.

(b) Gauss-Legendre quadrature level is 8 (129 points). Polynomial order is 7.

Figure 15: One dimensional stochastic gas dynamics Riemann problem: posteriors on the initial interface abscissa the posterior accelerated with gPC, with i-gPC and the exact one built with the analytical solution

Kullback-Leibler divergence on discontinuous solutions: at fixed P , for such solutions, the Kullback-Leibler divergence may increase as the L^2 projection error decreases (i.e., k increases). Let us now comment on the behaviour of i-gPC in the same context. The accu-

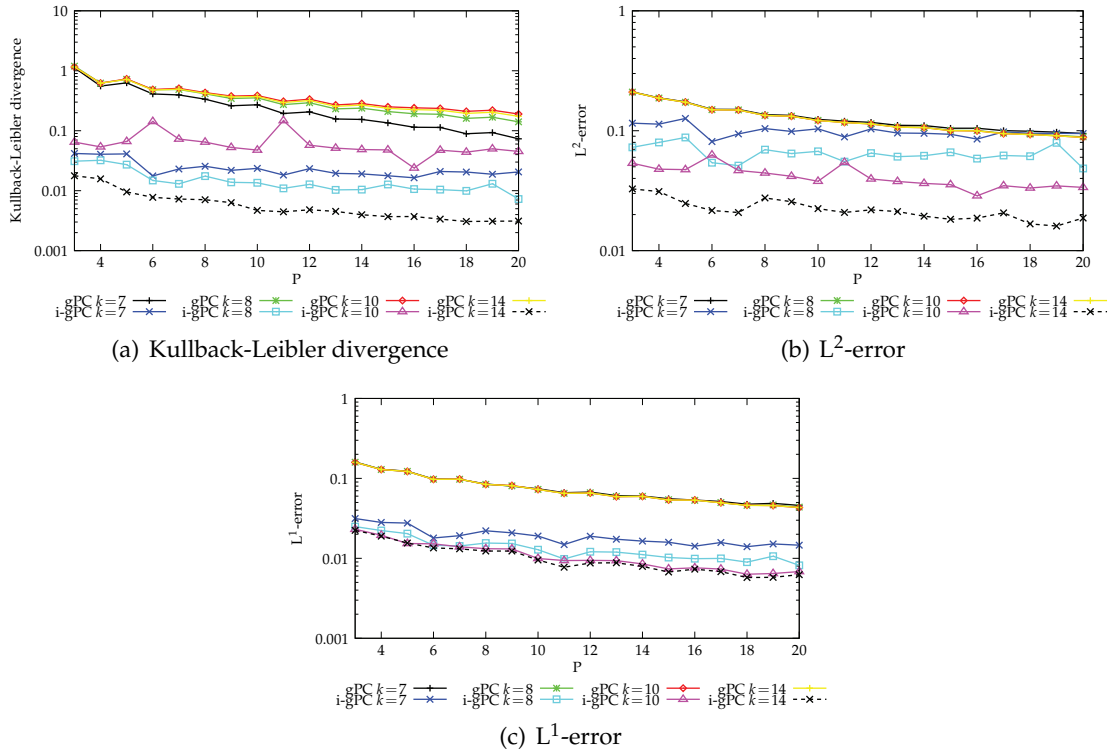


Figure 16: SOD test case: convergence of the Kullback-Leibler divergence, of the L^2 -error and of the L^1 -error with respect to the polynomial order P for different integration levels k from 6 to 14. The use of i-gPC improves the convergence in the Kullback-Leibler norm, in the L^1 norm and in the L^2 norm.

racy of the i-gPC approximations for fixed P and k is better than for gPC. The conclusion is that it is always better to use i-gPC compared to gPC, and this is the case in term of the Kullback-Leibler divergence, the L^1 norm and the L^2 norm. Finally, in Fig. 16, we notice that the increase in the numerical accuracy does not improve the accuracy of gPC whereas i-gPC allows an important gain making the most of numerical integration.

6 Conclusions

In this paper, we have tackled the resolution of inverse problem implying strongly non linear or discontinuous behaviours, namely systems of conservation laws (governing compressible gas dynamics). We first related the exponential L^2 -convergence of the forward approximation to the exponential convergence in terms of Kullback-Leibler divergence of the approximate posterior. In particular, we proved that under the assumption of uniform prior distribution, the convergence of the posterior, is at least twice as fast as the convergence rate of the forward model in the L^2 -sense. The Bayesian inference strategy has been developed in the framework of a stochastic spectral projection method. The

predicted convergence rates have been demonstrated for simple nonlinear inverse problems of varying smoothness. We furthermore suggested an efficient numerical approach for the Bayesian solution of inverse problems adapted to strongly nonlinear or discontinuous system responses. This comes with the improvement of the forward model that is adaptively approximated by an iterative generalized Polynomial Chaos-based representation. This new approach allows a gain with respect to gPC and accelerates the convergence of Bayesian inference. We demonstrated the efficiency of the new approach in the context of finite accuracy numerical quadrature rule. The new approach makes the inference more accurate and above all not misleading which is fundamental in practical and industrial applications.

References

- [1] R. Archibald, A. Gelb, R. Saxena and D. Xiu, Discontinuity detection in multivariate space for stochastic simulations, *J. Comput. Phys.*, 228(7) (2009), 2676–2689.
- [2] M. Arnst and R. Ghanem, Probabilistic equivalence and stochastic model reduction in multiscale analysis, *Comput. Methods Appl. Mech. Eng.*, 197(43-44) (2008), 3584–3592.
- [3] J. O. Berger, J. M. Bernardo and D. Sun, The formal definition of reference priors, *The Annals Stat.*, 37(2) (2009), 905–938.
- [4] Bojana V. Rosic, Anna Kucerová, Jan Sykora, Oliver Pajonk, Alexander Litvinenko and Hermann G. Matthies, Parameter identification in a probabilistic setting, *Eng. Struct.*, 50 (2013), 179–196.
- [5] R. H. Cameron and W. T. Martin, The orthogonal development of non-linear functionals in series of Fourier-Hermite functionals, *Annals Math.*, 48 (1947), 385–392.
- [6] Paul G. Constantine, Michael S. Eldred and Eric T. Phipps, Sparse pseudospectral approximation method, *Comput. Methods Appl. Mech. Eng.*, 229-232(0) (2012), 1–12.
- [7] Sonjoy Das, Roger Ghanem and James C. Spall, Asymptotic sampling distribution for polynomial chaos representation from data: a maximum entropy and fisher information approach, 30(5) (2008), 2207–2234.
- [8] C. Desceliers, R. Ghanem and C. Soize, Maximum likelihood estimation of stochastic chaos representations from experimental data, *Int. J. Numer. Methods Eng.*, 66(6) (2006), 978–1001.
- [9] B. Després et al., *Lois de Conservations Eulériennes, Lagrangiennes et Méthodes Numériques*, Volume 68, Springer Verlag, 2010.
- [10] D. Galbally, K. Fidkowski, K. Willcox and O. Ghattas, Non-linear model reduction for uncertainty quantification in large-scale inverse problems, *Int. J. Numer. Methods Eng.*, 81(12) (2010), 1581–1608.
- [11] Walter Gautschi, *Orthogonal Polynomials: Applications and Computation*, Volume 5, Oxford University Press, 1996.
- [12] Alan E. Gelfand and Adrian F. M. Smith, Sampling-based approaches to calculating marginal densities, *J. Am. Stat. Association*, 85(410) (1990), 398–409.
- [13] Stuart Geman and Donald Geman, Stochastic relaxation, Gibbs distributions, and the Bayesian restoration of images, *PAMI*, 6 (1984), 721–741.
- [14] M. I. Gerritsma, J.-B. van der Steen, P. Vos and G. E. Karniadakis, Time-dependent generalized polynomial chaos, *J. Comput. Phys.*, (2010), 8333–8363.
- [15] R. G. Ghanem and P. Spanos, *Stochastic Finite Elements: a Spectral Approach* (revised edition), Springer-Verlag, 2003.

- [16] Roger G. Ghanem and Alireza Doostan, On the construction and analysis of stochastic models: characterization and propagation of the errors associated with limited data, *J. Comput. Phys.*, 217(1) (2006), 63–81.
- [17] Roger G. Ghanem, Alireza Doostan and John Red-Horse, A probabilistic construction of model validation, *Comput. Methods Appl. Mech. Eng.*, 197(29-32) (2008), 2585–2595.
- [18] W. R. Gilks, S. Richardson and D. J. Spiegelhalter, *Markov Chain Monte Carlo in Practice*, Chapman & Hall, 1995.
- [19] S. Gottlieb, J. H. Jung and S. Kim, A review of David Gottlieb’s work on the resolution of the Gibbs phenomenon, *Commun. Comput. Phys.*, 9 (2011), 497–519.
- [20] D. Higdon, M. Kennedy, J. C. Cavendish, J. A. Cafo and R. D. Ryne, Combining field data and computer simulations for calibration and prediction, *SIAM J. Sci. Comput.*, 26 (2004), 448.
- [21] J. D. Jakeman, A. Narayan and X. Dongbin, Minimal multi-element stochastic collocation for uncertainty quantification of discontinuous functions, *J. Comput. Phys.*, 242 (2013), 790–808.
- [22] E. T. Jaynes, Prior probabilities, *Systems Science and Cybernetics*, *IEEE Transactions on*, 4(3) (1968), 227–241.
- [23] E. T. Jaynes, *Marginalization and Prior Probabilities*, *Bayesian Analysis in Econometrics and Statistics*, A. Zellner, ed., North-Holland Publishing Company, Amsterdam, 1980.
- [24] E. T. Jaynes, *Papers on Probability, Statistics and Statistical Physics*, Volume 50, Springer, 1989.
- [25] H. Jeffreys, An invariant form for the prior probability in estimation problems, *Proc. Roy. Soc. London Math. Phys. Sci.*, 186 (1946), 453–461.
- [26] M. Junk, Maximum entropy for reduced moment problems, *Math. Models Methods Appl. Sci.*, 10(7) (2000), 1001–1026.
- [27] J. Kaipio and E. Somersalo, *Statistical and Computational Inverse Problems*, Volume 160 of *Applied Mathematical Sciences*, Springer, 2005.
- [28] Andreas Keese, *Numerical Solution of Systems with Stochastic Uncertainties: a General Purpose Framework for Stochastic Finite Elements*, PhD thesis, Technische Universität Braunschweig, Mechanik-Zentrum, 2005.
- [29] M. C. Kennedy and A. O’Hagan, Bayesian calibration of computer models, *J. Royal Stat. Soc. Ser. B, (Statistical Methodology)*, 63(3) (2001), 425–464.
- [30] S. Kullback and R. A. Leibler, On information and sufficiency, *Annals Math. Stat.*, 22(1) (1951), 79–86.
- [31] O. Le Maitre, O. Knio, H. Najm and R. Ghanem, Uncertainty propagation using Wiener-Haar expansions, *J. Comput. Phys.*, 197 (2004), 28–57.
- [32] O. Le Maitre, M. Reagan, H. Najm, R. Ghanem and O. Knio, Multi-resolution analysis of Wiener-type uncertainty propagation schemes, *J. Comput. Phys.*, 197 (2004), 502–531.
- [33] O. P. Le Maître and Omar M. Knio, *Spectral Methods for Uncertainty Quantification with applications to Computational Fluid Dynamics*, *Scientific Computation*, Springer Netherlands, 2010.
- [34] J. Le Meitour, D. Lucor and J.-C. Chassaing, Adaptive piecewise polynomial chaos approaches: application to nonlinear aeroelastic flutter, in *ASME 2010 3rd Joint US-European Fluids Engineering Summer Meeting: Volume 1, Symposia–Parts A, B, and C*, pages 2957–2968, August 1-5 2010, Montreal, Canada, 2010.
- [35] F. Liese and I. Vajda, On divergences and informations in statistics and information theory, *Information Theory*, *IEEE Transactions on*, 52(10) (2006), 4394–4412.
- [36] D. Lucor, C. Enaux, H. Jourden and P. Sagaut, *Stochastic design optimization: application*

- to reacting flows and detonation, *Comput. Meth. Appl. Mech. Eng.*, 196(49-52) (2007), 5047–5062.
- [37] D. Lucor, J. Meyers and P. Sagaut, Sensitivity analysis of LES to subgrid-scale-model parametric uncertainty using Polynomial Chaos, *J. Fluid Mech.*, 585 (2007), 255–279.
- [38] D. Lucor, J. Witteveen, P. Constantine, D. Schiavazzi and G. Iaccarino, Comparison of adaptive uncertainty quantification approaches for shock wave-dominated flows, in *Proceedings of the Summer Program, Center for Turbulence Research, Stanford University*, 2013.
- [39] Xiang Ma and Nicholas Zabaras, An adaptive hierarchical sparse grid collocation algorithm for the solution of stochastic differential equations, *J. Comput. Phys.*, 228(8) (2009), 3084–3113.
- [40] Y. Marzouk and D. Xiu, A stochastic collocation approach to bayesian inference in inverse problems, *Commun. Comput. Phys.*, 2009.
- [41] Y. M. Marzouk and H. N. Najm, Dimensionality reduction and polynomial chaos acceleration of bayesian inference in inverse problems, *J. Comput. Phys.*, 228(6) (2009), 1862–1902.
- [42] Y. M. Marzouk, H. N. Najm and L. A. Rahn, Stochastic spectral methods for efficient bayesian solution of inverse problems, *J. Comput. Phys.*, 224(2) (2007), 560–586.
- [43] Youssef Marzouk and Dongbin Xiu, A stochastic collocation approach to Bayesian inference in inverse problems, *Commun. Comput. Phys.*, 6(4) (2009), 826–847.
- [44] Youssef M. Marzouk and Habib N. Najm, Dimensionality reduction and Polynomial Chaos acceleration of Bayesian inference in inverse problems, *J. Comput. Phys.*, 228(6) (2009), 1862–1902.
- [45] Youssef M. Marzouk, Habib N. Najm and Larry A. Rahn, Stochastic spectral methods for efficient Bayesian solution of inverse problems, *J. Comput. Phys.*, 224(2) (2007), 560–586.
- [46] L. Mathelin and O. P. Le Maître, A posteriori error analysis for stochastic finite element solutions of fluid flows with parametric uncertainties, *ECCOMAS CFD*, 2006.
- [47] H. Matthies and A. Keese, Galerkin methods for linear and nonlinear elliptic stochastic partial differential equations, *Comput. Meth. Appl. Mech. Eng.*, 192(12-16) (2005), 1295–1331.
- [48] L. R. Mead and N. Papanicolaou, Maximum entropy in the problem of moments, *J. Math. Phys.*, 25(8) (1984).
- [49] M. Meldi, P. Sagaut and D. Lucor, A stochastic view of isotropic turbulence decay, *J. Fluid Mech.*, 668 (2011), 351–362.
- [50] N. Metropolis, A. W. Rosenbluth, M. N. Rosenbluth, A. H. Teller and E. Teller, Equation of state calculations by fast computing machines, *J. Chem. Phys.*, 21 (1953), 1087–1092.
- [51] H. N. Najm O.P. Le Maître, O. M. Knio and R. G. Ghanem, A stochastic projection method for fluid flow i: basic formulation, *J. Comput. Phys.*, 173 (2001), 481–511.
- [52] M. S. Pinsker, Information and information stability of random variables and processes, *Holden-Day Series in Time Series Analysis*, 1960.
- [53] G. Poëtte, A. Birolleau and D. Lucor, Iterative generalized Polynomial Chaos approximations, *SIAM J. Sci. Comput.*, submitted, 2012.
- [54] G. Poëtte, B. Després and D. Lucor, Uncertainty quantification for systems of conservation laws, *J. Comput. Phys.*, 228(7) (2009), 2443–2467.
- [55] G. Poëtte, B. Després and D. Lucor, Adaptive hybrid spectral methods for stochastic systems of conservation laws, in A. Sequeira J. C. F. Pereira and J. M. C. Pereira, editors, *ECCOMAS CFD 2010 Proceedings of the V European Conference on Computational Fluid Dynamics*, Lisbon, Portugal, 2010.
- [56] G. Poëtte, B. Després and D. Lucor, Treatment of uncertain interfaces in compressible flows, *Comput. Meth. Appl. Math. Eng.*, 200(1-4) (2011), 284–308.

- [57] G. Poëtte, B. Després and D. Lucor, Uncertainty Propagation for Systems of Conservation Laws, High-Order Stochastic Spectral Methods, in Jan S. Hesthaven and Einar M. Rønquist, editors, Spectral and High Order Methods for Partial Differential Equations, Lecture Notes in Computational Science and Engineering, pages 293–307, ICOSAHOM '09 conference, June 22-26 2009, Trondheim, Norway, 2011.
- [58] G. Poëtte and D. Lucor, Non intrusive iterative stochastic spectral representation with application to compressible gas dynamics, J. Comput. Phys., 2011, DOI information: 10.1016/j.jcp.2011.12.038.
- [59] Poggi, Thorembey and Rodriguez, Velocity Measurements in turbulent gaseous mixtures induced by Richtmyer-Meshkov instability, Phys. Fluids, 10 (1998), 11.
- [60] C. P. Robert and G. Casella, Monte Carlo Statistical Methods, Springer-Verlag, New York, 2nd edition, 2004.
- [61] C. P. Robert, The Bayesian Choice: From Decision-Theoretic Foundations to Computational Implementation, Springer Verlag, 2007.
- [62] D. Serre, Systèmes Hyperboliques de Lois de Conservation, partie I, Diderot, 1996, Paris.
- [63] D. Serre, Systèmes Hyperboliques de Lois de Conservation, partie II, Diderot, 1996, Paris.
- [64] F. Simon, P. Guillen, P. Sagaut and D. Lucor, A gPC-based approach to uncertain transonic aerodynamics, Comput. Methods Appl. Mech. Eng., 199(17-20) (2010), 1091–1099.
- [65] A. Tarantola, Inverse Problem Theory—Methods for Data Fitting and Model Parameter Estimation, Elsevier, 1987.
- [66] A. Tarantola, Inverse Problem Theory and Methods for Model Parameter Estimation, SIAM: Philadelphia, 2005.
- [67] M. Tatang, W. Pan, R. Prinn and G. McRae, An efficient method for parametric uncertainty analysis of numerical geophysical models, J. Geophys. Res., 102 (1997), 21925–21932.
- [68] E. F. Toro, Riemann Solver and Numerical Methods for Fluid Dynamics, Springer-Verlag, 1997.
- [69] J. Tryoen, Adaptive anisotropic stochastic discretization schemes for uncertain conservation laws, in ASME–FEDSM Proceedings, Montreal, Canada, 2010.
- [70] Vetter and Sturtevant, Experiments on the Richtmyer-Meshkov instability of an air/SF6 interface, Shock Waves, 4 (1995), 247–252.
- [71] P. Vos, Time Dependent Polynomial Chaos, Master of science thesis, Delft University of Technology, Faculty of Aerospace Engineering, 2006.
- [72] X. Wan and G. E. Karniadakis, An adaptive multi-element generalized polynomial chaos method for stochastic differential equations, J. Comput. Phys., 209 (2005), 617–642.
- [73] X. Wan and G. E. Karniadakis, An adaptive multi-element generalized polynomial chaos method for stochastic differential equations, J. Comput. Phys., 209(2) (2005), 617–642.
- [74] X. Wan and G. E. Karniadakis, Multi-element generalized Polynomial Chaos for arbitrary probability measures, SIAM J. Sci. Comput., 28(3) (2006), 901–928.
- [75] X. Wan and G. E. Karniadakis, Stochastic heat transfer enhancement in a grooved channel, J. Fluid Mech., 565 (2006), 255–278.
- [76] Xiaoliang Wan and George Em Karniadakis, Error control in multi-element generalized Polynomial Chaos method for elliptic problems with random coefficients, Commun. Comput. Phys., 5(2-4) (2009), 793–820.
- [77] Jingbo Wang and Nicholas Zabaras, Hierarchical bayesian models for inverse problems in heat conduction, Inverse Problems, 21 (2005), 183–206.
- [78] N. Wiener, The homogeneous chaos, Amer. J. Math., 60(4) (1938), 897–936.
- [79] N. Wiener, The homogeneous chaos, Amer. J. Math., 60 (1938), 897–936.

- [80] J. Witteveen and G. Iaccarino, Subcell resolution in simplex stochastic collocation for spatial discontinuities, *J. Comput. Phys.*, 251 (2013), 17–52.
- [81] D. Xiu and G. E. Karniadakis, The Wiener-Askey Polynomial Chaos for stochastic differential equations, *SIAM J. Sci. Comput.*, 24 (2002), 619–644.
- [82] D. Xiu, D. Lucor, C.-H. Su and G. E. Karniadakis, Stochastic modeling of flow-structure interactions using generalized Polynomial Chaos, *J. Fluid Eng.*, 124(1) (2002), 51–59.
- [83] Dongbin Xiu, *Numerical Methods for Stochastic Computations: A Spectral Method Approach*, Princeton Univ. Press, 2010.
- [84] R. Yang and J. O. Berger, *A Catalog of Noninformative Priors*, Institute of Statistics and Decision Sciences, Duke University, 1996.